8 Second-Harmonic Generation and Parametric Oscillation

8.0 INTRODUCTION

In Chapter 1 we considered the propagation of electromagnetic radiation in linear media in which the polarization is proportional to the electric field that induces it. In this chapter we consider some of the consequences of the nonlinear dielectric properties of certain classes of crystals in which, in addition to the linear response, a field produces a polarization proportional to the square of the field.

The nonlinear response can give rise to exchange of energy between a number of electromagnetic fields of different frequencies. Two of the most important applications of this phenomenon are: (1) second-harmonic generation in which part of the energy of an optical wave of frequency ω propagating through a crystal is converted to that of a wave at 2ω, and (2) parametric oscillation in which a strong pump wave at ω_3 causes the simultaneous generation in a nonlinear crystal of radiation at ω_1 and ω_2, where $\omega_3 = \omega_1 + \omega_2$. These will be treated in detail in this chapter.

8.1 ON THE PHYSICAL ORIGIN OF NONLINEAR POLARIZATION

The optical polarization of dielectric crystals is due mostly to the outer, loosely bound valence electrons that are displaced by the optical field. Denoting the electron deviation from the equilibrium position by x and the density of electrons by N, the polarization p is given by

$$p(t) = -Nex(t)$$

In symmetric crystals the potential energy of an electron must reflect the crystal symmetry, so that, using a one-dimensional analog, it can be written as

$$V(x) = \frac{m}{2}\omega_0^2 x^2 + \frac{m}{4}Bx^4 + \cdots \tag{8.1-1}$$

where ω_0^2 and B are constants[1] and m is the electron mass. Because of the symmetry $V(x)$ contains only even powers of x, so $V(-x) = V(x)$. The restoring force on an electron is

$$F = -\frac{\partial V}{\partial x} = -m\omega_0^2 x - mBx^3 \tag{8.1-2}$$

and is zero at the equilibrium position $x = 0$.

The linear polarization of crystals in which the polarization is proportional to the electric field is accounted for by the first term in (8.1-1). To see this, consider a "low" frequency electric field $E(t)$—that is, a field whose Fourier components are at frequencies small compared to ω_0. The excursion $x(t)$ caused by this field is found by equating the total force on the electron to zero[2]

$$-eE(t) - m\omega_0^2 x(t) = 0$$

so that

$$x(t) = -\frac{e}{m\omega_0^2}E(t) \tag{8.1-3}$$

thus resulting in a polarization $p(t) = -Nex(t)$, which is instantaneously proportional to the field.

Now in an asymmetric crystal in which the condition $V(x) = V(-x)$ is no longer fulfilled, the potential function can contain odd powers of x and thus

$$V(x) = \frac{m\omega_0^2}{2}x^2 + \frac{m}{3}Dx^3 + \cdots \tag{8.1-4}$$

which corresponds to a restoring force on the electron

$$F = -\frac{\partial V(x)}{\partial x} = -(m\omega_0^2 x + mDx^2 + \cdots) \tag{8.1-5}$$

An examination of (8.1-5) reveals that a positive excursion ($x > 0$) results in a larger restoring force, assuming $D > 0$, than does the same excursion

---

[1]The constant ω_0 was found in Section 5.4 to correspond to the resonance frequency of the electronic oscillator.

[2]The "low" frequency assumption makes it possible to neglect the acceleration term $m\,d^2x/dt^2$ in the force equation.

in the opposite direction. It follows immediately that if the electric force on the electron is positive ($E < 0$), the induced polarization is smaller than when the field direction is reversed. This situation is depicted in Figure 8-1.

Next consider an alternating electric field at an (optical) frequency ω applied to the crystal. In a linear crystal the induced polarization will be proportional, at any moment, to the field, resulting in a polarization oscillating at ω as shown in Figure 8-2(a). In a nonlinear crystal we can use Figure 8-1(b) to obtain the induced polarization corresponding to a given field and then plot it (vertically) as in Figure 8-2(b). The result is a polarization wave in which the stiffer restoring force at $x > 0$ results in positive peaks (b), which are smaller than the negative ones (b'). A Fourier analysis of the nonlinear polarization wave in Figure 8-2(b) shows that it contains the second harmonic of ω as well as an average (dc) term. The average, fundamental, and second-harmonic components are plotted in Figure 8-3.

To relate the nonlinear polarization formally to the inducing field, we use Equation (8.1-5) for the restoring force and take the driving electric field

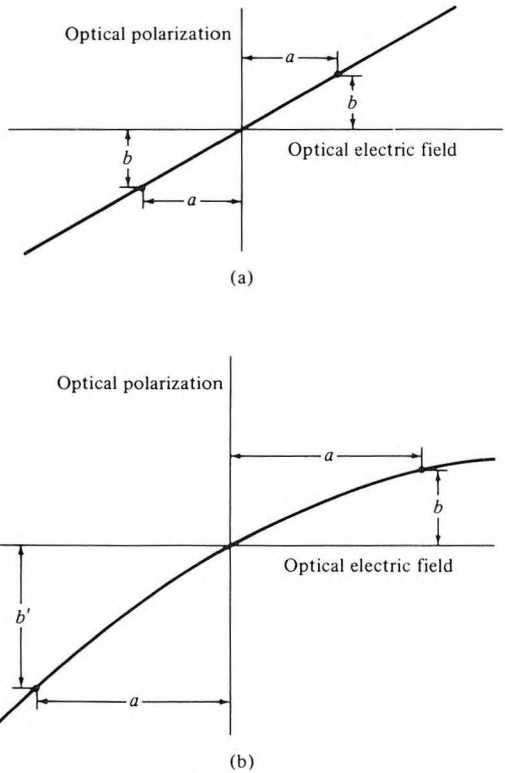

Figure 8-1 Relation between induced polarization and the electric field causing it; (a) in a linear dielectric and (b) in a crystal lacking inversion symmetry.

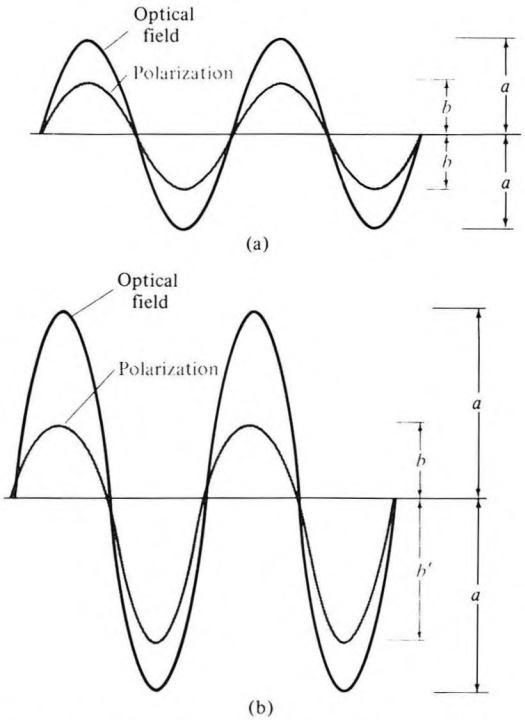

Figure 8-2 An applied sinusoidal electric field and the resulting polarization; (a) in a linear crystal and (b) in a crystal lacking inversion symmetry.

as $E^{(\omega)} \cos \omega t$. The equation of motion of the electron $F = m\ddot{x}$ is then

$$\frac{d^2x(t)}{dt^2} + \sigma \frac{dx(t)}{dt} + \omega_0^2 x(t) + Dx^2(t) = -\frac{eE^{(\omega)}}{2m}(e^{i\omega t} + e^{-i\omega t}) \qquad (8.1\text{-}6)$$

where, as in (5.4-1), we account for the losses by a frictional force $-m\sigma\dot{x}$. An inspection of (8.1-6) shows that the term Dx^2 gives rise to a component oscillating at 2ω, so we assume the solution for $x(t)$ in the form[3]

$$x(t) = \tfrac{1}{2}(q_1 e^{i\omega t} + q_2 e^{2i\omega t} + \text{c.c.}) \qquad (8.1\text{-}7)$$

where c.c. stands for "complex conjugate."

Substituting the last expression into (8.1-6) gives

$$-\frac{\omega^2}{2}(q_1 e^{i\omega t} + \text{c.c.}) - 2\omega^2(q_2 e^{2i\omega t} + \text{c.c.}) + \frac{i\omega\sigma}{2}(q_1 e^{i\omega t} - \text{c.c.})$$

$$+ i\omega\sigma(q_2 e^{2i\omega t} - \text{c.c.}) + \frac{\omega_0^2}{2}(q_1 e^{i\omega t} + q_2 e^{2i\omega\sigma} + \text{c.c.})$$

[3]Here we must use the real form of $x(t)$ instead of the complex one since, as discussed in Section 1.1, the differential equation involves x^2.

$$+ \frac{D}{4}(q_1^2 e^{2i\omega t} + q_2^2 e^{4i\omega t} + q_1 q_1^* + 2q_1 q_2 e^{3i\omega t}$$

$$+ 2q_1 q_2^* e^{-i\omega t} + q_2 q_2^* + \text{c.c.}) = \frac{-eE^{(\omega)}}{2m}(e^{i\omega t} + \text{c.c.}) \qquad (8.1\text{-}8)$$

If (8.1-8) is to be valid for all times t, the coefficients of $e^{\pm i\omega t}$ and $e^{\pm 2i\omega t}$ on both sides of the equation must be equal. Equating first the coefficients of $e^{i\omega t}$, assuming that $|Dq_2| \ll [(\omega_0^2 - \omega^2)^2 + \omega^2\sigma^2]^{1/2}$, gives

$$q_1 = -\frac{eE^{(\omega)}}{m}\frac{1}{(\omega_0^2 - \omega^2) + i\omega\sigma} \qquad (8.1\text{-}9)$$

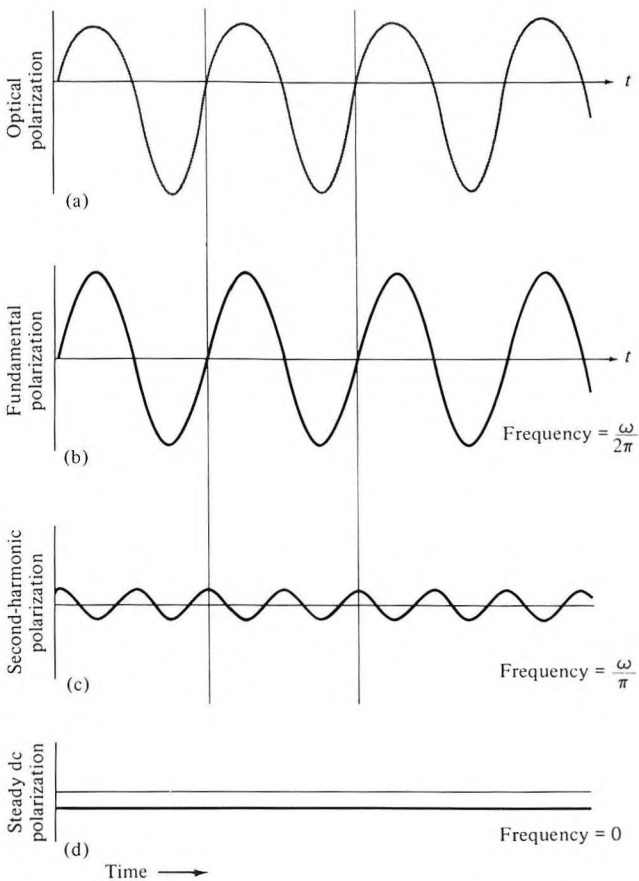

Figure 8-3 Analysis of the nonlinear polarization wave (a) of Figure 8.2 (b) shows that it contains components oscillating at (b) the same frequency (ω) as the wave inducing it, (c) twice that frequency (2ω), and (d) an average (dc) negative component.

The polarization at ω is related to the electronic deviation at ω by

$$p^{(\omega)}(t) = -\frac{Ne}{2}(q_1 e^{i\omega t} + \text{c.c.})$$

$$\equiv \frac{\epsilon_0}{2}[\chi(\omega)E^{(\omega)}e^{i\omega t} + \text{c.c.}] \tag{8.1-10}$$

where $\chi(\omega)$ is thus the linear susceptibility defined by (5.4-8). By using (8.1-9) in (8.1-10) and solving for $\chi(\omega)$, we obtain

$$\chi(\omega) = \frac{Ne^2}{m\epsilon_0[(\omega_0^2 - \omega^2) + i\omega\sigma]} \tag{8.1-11}$$

We now proceed to solve for the amplitude q_2 of the electronic motion at 2ω. Equating the coefficients of $e^{2i\omega t}$ on both sides of (8.1-8) leads to

$$q_2(-4\omega^2 + 2i\omega\sigma + \omega_0^2) = -\tfrac{1}{2}Dq_1^2$$

and, after substituting the solution (8.1-9) for q_1, we obtain

$$q_2 = \frac{-De^2(E^{(\omega)})^2}{2m^2[(\omega_0^2 - \omega^2) + i\omega\sigma]^2(\omega_0^2 - 4\omega^2 + 2i\omega\sigma)} \tag{8.1-12}$$

In a manner similar to (8.1-10), the nonlinear polarization at 2ω is

$$p^{(2\omega)}(t) = -\frac{Ne}{2}(q_2 e^{2i\omega t} + \text{c.c.})$$

$$\equiv \tfrac{1}{2}\{d^{(2\omega)}[E^{(\omega)}]^2 e^{2i\omega t} + \text{c.c.}\} \tag{8.1-13}$$

The second of equations (8.1-13) defines the *nonlinear optical coefficient* $d^{(2\omega)}$. If we denote the complex amplitude of the polarization as $P^{(2\omega)}$ we have, from (8.1-13),

$$p^{(2\omega)}(t) = \tfrac{1}{2}[P^{(2\omega)}e^{2i\omega t} + \text{c.c.}]$$

and

$$P^{(2\omega)} = d^{(2\omega)}E^{(\omega)}E^{(\omega)} \tag{8.1-14}$$

that is, $d^{(2\omega)}$ is the ratio of the (complex) amplitude of the polarization at 2ω to the square of the fundamental amplitude. Substituting (8.1-12) for q_2 in (8.1-13), then solving for $d^{(2\omega)}$, results in

$$d^{(2\omega)} = \frac{DNe^3}{2m^2[(\omega_0^2 - \omega^2) + i\omega\sigma]^2(\omega_0^2 - 4\omega^2 + 2i\omega\sigma)} \tag{8.1-15}$$

Using (8.1-11) we can rewrite (8.1-15) as

$$d^{(2\omega)} = \frac{mD[\chi^{(\omega)}]^2\chi^{(2\omega)}\epsilon_0^3}{2N^2e^3} \tag{8.1-16}$$

Equation (8.1-16) is important since it relates the nonlinear optical coefficient d to the linear optical susceptibilities χ and to the anharmonic coefficient D.

Estimates based on this relation are quite successful in predicting the size of the coefficient d in a large variety of crystals; see References [1, 2].

Relation (8.1-14) is scalar. In actual crystals we must consider the symmetry so that the second harmonic polarization along, say, the x direction, is related to the electric field at ω by a third rank tensor d_{ijk}.

$$P_x^{(2\omega)} = d_{xxx}^{(2\omega)}E_x^{(\omega)}E_x^{(\omega)} + d_{xyy}^{(2\omega)}E_y^{(\omega)}E_y^{(\omega)} + d_{xzz}^{(2\omega)}E_z^{(\omega)}E_z^{(\omega)} + 2d_{xzy}^{(2\omega)}E_z^{(\omega)}E_y^{(\omega)} + 2d_{xzx}^{(2\omega)}E_z^{(\omega)}E_x^{(\omega)} + 2d_{xxy}^{(2\omega)}E_x^{(\omega)}E_y^{(\omega)} \quad (8.1\text{-}17)$$

Similar relations give $P_y^{(2\omega)}$ and $P_z^{(2\omega)}$. Considerations of crystal symmetry reduce the number of nonvanishing $d_{ijk}^{(2\omega)}$ coefficients—or, in certain cases to be discussed in the following, cause them to vanish altogether. Table 8-1 lists the nonlinear coefficients of a number of crystals.

Crystals are usually divided into two main groups, depending on whether the crystal structure remains unchanged upon inversion (that is, replacing the coordinate $\mathbf{r}$ by $-\mathbf{r}$) or not. Crystals belonging to the first group are called centrosymmetric, whereas crystals of the second group are called noncentrosymmetric [3]. In Figure 8-4 we show the crystal structure of NaCl, a centrosymmetric crystal; an example of a crystal lacking inversion symmetry (noncentrosymmetric) is provided by crystals of the ZnS (zinc blende) class such as GaAs, CdTe, and others. The crystal structure of ZnS is shown in Figure 8-5. The lack of inversion symmetry is evident in the projection of the atomic positions given by Figure 8-6.

In crystals possessing an inversion symmetry, all the nonlinear optical coefficients $d_{ijk}^{(2\omega)}$ must be zero. This follows directly from the relation

$$P_i^{(2\omega)} = \sum_{j,k=x,y,z} d_{ijk}^{(2\omega)}E_j^{(\omega)}E_k^{(\omega)} \quad (8.1\text{-}18)$$

which is a compact notation for relation (8.1-17). Let us reverse the direction of the electric field so that in (8.1-18) $E_j^{(\omega)}$ becomes $-E_j^{(\omega)}$ and $E_k^{(\omega)}$ becomes $-E_k^{(\omega)}$. Since the crystal is centrosymmetric, the reversed field "sees" a crystal identical to the original one so that the polarization produced by it must bear the same relationship to the field as originally; that is, the new polarization is $-P_i^{(2\omega)}$. Since the new polarization and the electric field causing it are still related by (8.1-18), we have

$$-P_i^{(2\omega)} = \sum_{j,k} d_{ijk}^{(2\omega)}(-E_j^{(\omega)})(-E_k^{(\omega)}) \quad (8.1\text{-}19)$$

Equations (8.1-18) and (8.1-19) can hold simultaneously only if the coefficients $d_{ijk}^{(2\omega)}$ are all zero. We may thus summarize: *In crystals possessing an inversion symmetry there is no second-harmonic generation.*

In the actual practice and design of experiments involving second-harmonic generation or any second-order nonlinear optics in general, it is crucial to take into account the vectorial nature of the interaction and the tensorial aspect of the d_{ijk} coefficients. A tabulation of the symmetry properties of these coefficients is included in [12] as well as a detailed example of their

Table 8-1 The Nonlinear Optical Coefficients of a Number of Crystals*

Crystal	$d_{ijk}^{(2\omega)}$ in Units of $1/9 \times 10^{-22}$ MKS
$LiIO_3$	$d_{15} = 4.4$
$NH_4H_2PO_4$	$d_{36} = 0.45$
(ADP)	$d_{14} = 0.50 \pm 0.02$
KH_2PO_4	$d_{36} = 0.45 \pm 0.03$
(KDP)	$d_{14} = 0.35$
KD_2PO_4	$d_{36} = 0.42 \pm 0.02$
	$d_{14} = 0.42 \pm 0.02$
KH_2ASO_4	$d_{36} = 0.48 \pm 0.03$
	$d_{14} = 0.51 \pm 0.03$
Quartz	$d_{11} = 0.37 \pm 0.02$
$AlPO_4$	$d_{11} = 0.38 \pm 0.03$
ZnO	$d_{33} = 6.5 \pm 0.2$
	$d_{31} = 1.95 \pm 0.2$
	$d_{15} = 2.1 \pm 0.2$
CdS	$d_{33} = 28.6 \pm 2$
	$d_{31} = 30 \pm 10$
	$d_{36} = 33$
GaP	$d_{14} = 80 \pm 14$
GaAs	$d_{14} = 72$
$BaTiO_3$	$d_{33} = 6.4 \pm 0.5$
	$d_{31} = 18 \pm 2$
	$d_{15} = 17 \pm 2$
$LiNbO_3$	$d_{15} = 4.4$
	$d_{22} = 2.3 \pm 1.0$
Te	$d_{11} = 517$
Se	$d_{11} = 130 \pm 30$
$Ba_2NaNb_5O_{15}$	$d_{33} = 10.4 \pm 0.7$
	$d_{32} = 7.4 \pm 0.7$
Ag_3AsS_3	$d_{22} = 22.5$
(proustite)	$d_{36} = 13.5$
CdSe	$d_{31} = 22.5 \pm 3$
$CdGeAs_2$	$d_{36} = 363 \pm 70$
$AgGaSe_2$	$d_{36} = 27 \pm 3$
$AgSbS_3$	$d_{36} = 9.5$
ZnS	$d_{36} = 13$

*Some authors define the nonlinear coefficient d by $P = \epsilon_0 dE^2$ rather than by the relation $P = dE^2$ used here.

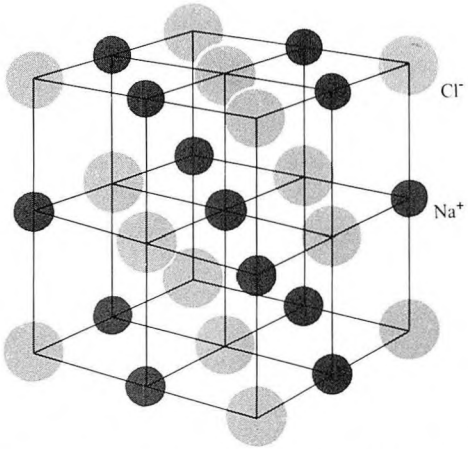

Figure 8-4 The crystal structure of NaCl. The crystal is centrosymmetric, since an inversion of any ion about the central Na^+ ion, as an example, leaves the crystal structure unchanged.

use in the case of KH_2PO_4. Alternatively we can generate these "symmetry tables" by replacing rows by columns in Table 9-1, i.e., by applying the transformation rule $d_{ij} \leftrightarrow r_{ji}$ to generate the 3×6 d_{ij} matrices from the 6×3 r_{ji} matrices. In the following sections we will employ a simplified scalar approach that, although retaining most of the physical considerations, needs to be supplemented in practice by vectorial considerations.

As an example that illustrates this point, consider a second-harmonic generation experiment in KH_2PO_4 (KDP). The incident beam at ω propagates along the crystal z (optic) axis and is polarized along the x or y axis or some intermediate direction between the two. Since second-harmonic generation in KDP (see Table 16.1 in Reference [12] for class $\bar{4}2m$ crystals) is described

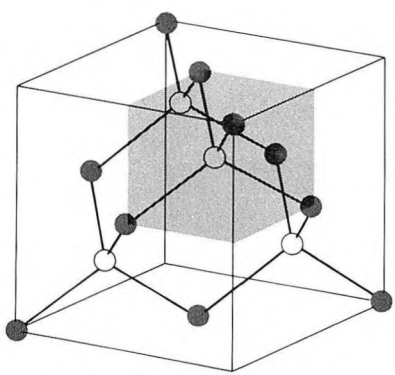

Figure 8-5 The crystal structure of cubic zinc sulfide.

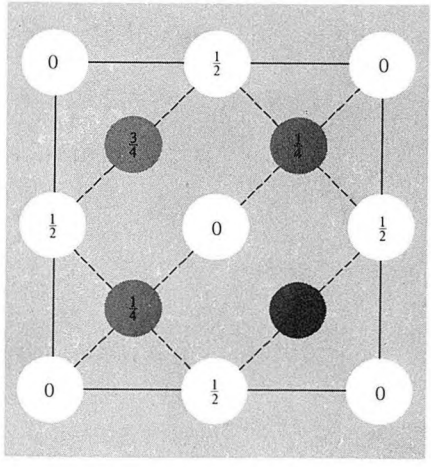

Figure 8-6 The atomic positions in the unit cell of ZnS projected on a cube face. The fractions denote height above base in units of a cube edge. The dark spheres correspond to zinc (or sulfur) atoms and are situated on a face-centered cubic (fcc) lattice, and the white spheres correspond to sulfur (or zinc) atoms and are situated on another fcc lattice displayed by $(\frac{1}{4}, \frac{1}{4}, \frac{1}{4})$ from the first one. Note the lack of inversion symmetry.

uniquely by

$$\begin{aligned} P_x^{(2\omega)} &= d_{xyz}E_y^{(\omega)}E_z^{(\omega)} \qquad (d_{xyz} = d_{14}) \\ P_y^{(2\omega)} &= d_{yxz}E_x^{(\omega)}E_z^{(\omega)} \qquad (d_{yxz} = d_{25}) \\ P_z^{(2\omega)} &= d_{zxy}E_x^{(\omega)}E_y^{(\omega)} \qquad (d_{zxy} = d_{36}) \end{aligned} \tag{8.1-19a}$$

our choice of propagation direction is such that $E_z^{(\omega)} = 0$. This results in the production of only $P_z^{(2\omega)}$. This polarization cannot, however, radiate a wave at 2ω propagating along the z axis, since the field E (more exactly D) must be normal to the propagation direction. We thus must choose a propagation direction at some, hopefully large, angle with respect to the z axis. The choice of this direction is dictated by "phase-matching" considerations as discussed in Section 8.3.

It follows, by a direct extension of (8.1-19), that if the optical field at a point $\mathbf{r}$ consists of two beams

$$e(t) = \mathrm{Re}[\mathbf{E}^{(\omega_1)}e^{i\omega_1 t} + \mathbf{E}^{(\omega_2)}e^{i\omega_2 t}] \tag{8.1-20}$$

there is induced in the material a polarization at the sum frequency $\omega_1 + \omega_2$

$$p_i^{(\omega_1+\omega_2)} = \mathrm{Re}[\, d_{ijk}^{(\omega=\omega_1+\omega_2)}E_j^{(\omega_1)}E_k^{(\omega_2)}e^{i(\omega_1+\omega_2)t}] \tag{8.1-21}$$

as well as at the difference frequency $\omega_1 - \omega_2$

$$p_i^{(\omega_1-\omega_2)} = \mathrm{Re}[\, d_{ijk}^{(\omega=\omega_1-\omega_2)}E_j^{(\omega_1)}(E_k^{(\omega_2)})^* e^{i(\omega_1-\omega_2)t}] \tag{8.1-22}$$

It follows that the complex amplitude of the induced polarization is related

to those of the inducing fields according to

$$P_i^{(\omega_1+\omega_2)} = d_{ijk}^{(\omega=\omega_1+\omega_2)} E_j^{(\omega_1)} E_k^{(\omega_2)}$$
$$P_i^{(\omega_1-\omega_2)} = d_{ijk}^{(\omega=\omega_1-\omega_2)} E_j^{(\omega_1)} (E_k^{(\omega_2)})^* \qquad (8.1\text{-}23)$$

The material constants $d_{ijk}^{(\omega=\omega_1+\omega_2)}$ and $d_{ijk}^{(\omega=\omega_1-\omega_2)}$ are, in general, not equal to each other since the physical processes contributing to the nonlinear polarization are usually dependent on the frequencies involved.

8.2 FORMALISM OF WAVE PROPAGATION IN NONLINEAR MEDIA

In this section we derive the equations governing the propagation of electromagnetic waves in nonlinear media. These equations will then be used to describe second-harmonic generation and parametric oscillation.

The starting point is Maxwell's equations (1.2-1), (1.2-2):

$$\nabla \times \mathbf{h} = \mathbf{i} + \frac{\partial \mathbf{d}}{\partial t}$$
$$\nabla \times \mathbf{e} = -\mu \frac{\partial \mathbf{h}}{\partial t} \qquad (8.2\text{-}1)$$

and

$$\mathbf{d} = \epsilon_0 \mathbf{e} + \mathbf{p}$$
$$\mathbf{i} = \sigma \mathbf{e} \qquad (8.2\text{-}2)$$

where σ is the conductivity. If we separate the total polarization $\mathbf{p}$ into its linear and nonlinear portions according to

$$\mathbf{p} = \epsilon_0 \chi_e \mathbf{e} + \mathbf{p}_{NL} \qquad (8.2\text{-}3)$$

the first of equations (8.2-1) becomes

$$\nabla \times \mathbf{h} = \sigma \mathbf{e} + \epsilon \frac{\partial \mathbf{e}}{\partial t} + \frac{\partial}{\partial t} \mathbf{p}_{NL} \qquad (8.2\text{-}4)$$

with $\epsilon \equiv \epsilon_0(1 + \chi_e)$. Taking the curl of both sides of the second of (8.2-1), using the vector identity,

$$\nabla \times \nabla \times \mathbf{e} = \nabla\nabla\cdot\mathbf{e} - \nabla^2\mathbf{e}$$

From (8.2-4) and taking $\nabla\cdot\mathbf{e} = 0$, we get

$$\nabla^2 \mathbf{e} = \mu\sigma \frac{\partial \mathbf{e}}{\partial t} + \mu\epsilon \frac{\partial^2 \mathbf{e}}{\partial t^2} + \mu \frac{\partial^2}{\partial t^2} \mathbf{p}_{NL} \qquad (8.2\text{-}5)$$

Next we go over to a scalar notation and rewrite (8.2-5) as

$$\nabla^2 e = \mu\sigma \frac{\partial e}{\partial t} + \mu\epsilon \frac{\partial^2 e}{\partial t^2} + \mu \frac{\partial^2}{\partial t^2} p_{NL}(\mathbf{r}, t) \qquad (8.2\text{-}6)$$

where we assumed, for simplicity, that $\mathbf{p}_{NL}$ is parallel to $\mathbf{e}$. Let us limit our consideration to a field made up of three plane waves propagating in the z direction with frequencies ω_1, ω_2, and ω_3 according to

$$\begin{aligned} e^{(\omega_1)}(z, t) &= \tfrac{1}{2}[E_1(z)e^{i(\omega_1 t - k_1 z)} + \text{c.c.}] \\ e^{(\omega_2)}(z, t) &= \tfrac{1}{2}[E_2(z)e^{i(\omega_2 t - k_2 z)} + \text{c.c.}] \\ e^{(\omega_3)}(z, t) &= \tfrac{1}{2}[E_3(z)e^{i(\omega_3 t - k_3 z)} + \text{c.c.}] \end{aligned} \tag{8.2-7}$$

Then the total instantaneous field is

$$e = e^{(\omega_1)}(z, t) + e^{(\omega_2)}(z, t) + e^{(\omega_3)}(z, t) \tag{8.2-8}$$

Next we substitute (8.2-8), using (8.2-7), into the wave equation (8.2-6) and separate the resulting equation into three equations, each containing only terms oscillating at one of the three frequencies. The nonlinear polarization $p_{NL}(\mathbf{r}, t)$ in (8.2-6) contains, according to (8.1-21) and (8.1-22), the terms

$$\text{Re}[d^{(\omega_1+\omega_2)}E_1E_2e^{i[(\omega_1+\omega_2)t-(k_1+k_2)z]}]$$

or

$$\text{Re}[d^{(\omega_3-\omega_2)}E_3E_2^*e^{i[(\omega_3-\omega_2)t-(k_3-k_2)z]}]$$

These oscillate at the new frequencies $(\omega_1 + \omega_2)$ and $(\omega_3 - \omega_2)$ and, in general being nonsynchronous, will not be able to drive the oscillation at ω_1, ω_2, or ω_3. An exception to the last statement is the case when

$$\omega_3 = \omega_1 + \omega_2 \tag{8.2-9}$$

In this case the term

$$\mu d \frac{\partial^2}{\partial t^2} E_1E_2e^{i[(\omega_1+\omega_2)t-(k_1+k_2)z]}$$

oscillates at $\omega_1 + \omega_2 = \omega_3$ and can thus act as a source for the wave at ω_3. In physical terms, we have power flow from the fields at ω_1 and ω_2 into that at ω_3, or vice versa. Assuming that (8.2-9) holds, we return to (8.2-6) and, writing it for the oscillation at ω_1, obtain

$$\begin{aligned} \nabla^2 e^{(\omega_1)} = {} & \mu\sigma_1 \frac{\partial e^{(\omega_1)}}{\partial t} + \mu\epsilon_1 \frac{\partial^2 e^{(\omega_1)}}{\partial t^2} \\ & + \mu d \frac{\partial^2}{\partial t^2}\left[\frac{E_3(z)E_2^*(z)}{2} e^{i[(\omega_3-\omega_2)t-(k_3-k_2)z]} + \text{c.c.}\right] \end{aligned} \tag{8.2-10}$$

Next we observe that, in view of (8.2-7),

$$\begin{aligned} \nabla^2 e^{(\omega_1)} &= \frac{1}{2}\frac{\partial^2}{\partial z^2}[E_1(z)e^{i(\omega_1 t - k_1 z)} + \text{c.c.}] \\ &= -\frac{1}{2}\left[k_1^2 E_1(z) + 2ik_1 \frac{dE_1(z)}{dz}\right] e^{i(\omega_1 t - k_1 z)} + \text{c.c.} \end{aligned}$$

where we assumed that

$$\left| k_1 \frac{dE_1(z)}{dz} \right| \gg \left| \frac{d^2E_1(z)}{dz^2} \right| \tag{8.2-11}$$

If we use (8.2-9) and (8.2-10), and take $\partial/\partial t = i\omega_1$, we obtain

$$\begin{aligned} -\frac{1}{2}\left[k_1^2 E_1(z) + 2ik_1 \frac{dE_1(z)}{dz} \right] e^{i(\omega_1 t - k_1 z)} + \text{c.c.} \\ = [i\omega_1 \mu\sigma_1 - \omega_1^2 \mu\epsilon_1] \left[\frac{E_1(z)}{2} e^{i(\omega_1 t - k_1 z)} \right] + \text{c.c.} \\ - \left[\frac{\omega_1^2 \mu d}{2} E_3(z) E_2^*(z) e^{i[\omega_1 t - (k_3 - k_2)z]} + \text{c.c.} \right] \end{aligned} \tag{8.2-12}$$

Recognizing that $k_1^2 = \omega_1^2 \mu\epsilon_1$, we can rewrite (8.2-12) after multiplying all the terms by

$$\frac{i}{k_1} \exp(-i\omega_1 t + ik_1 z)$$

as

$$\frac{dE_1}{dz} = -\frac{\sigma_1}{2}\sqrt{\frac{\mu}{\epsilon_1}}\, E_1 - \frac{i\omega_1}{2}\sqrt{\frac{\mu}{\epsilon_1}}\, dE_3 E_2^* e^{-i(k_3 - k_2 - k_1)z}$$

and, similarly,

$$\begin{aligned} \frac{dE_2^*}{dz} &= -\frac{\sigma_2}{2}\sqrt{\frac{\mu}{\epsilon_2}}\, E_2^* + \frac{i\omega_2}{2}\sqrt{\frac{\mu}{\epsilon_2}}\, dE_1 E_3^* e^{-i(k_1 - k_3 + k_2)z} \\ \frac{dE_3}{dz} &= -\frac{\sigma_3}{2}\sqrt{\frac{\mu}{\epsilon_3}}\, E_3 - \frac{i\omega_3}{2}\sqrt{\frac{\mu}{\epsilon_3}}\, dE_1 E_2 e^{-i(k_1 + k_2 - k_3)z} \end{aligned} \tag{8.2-13}$$

for the fields at ω_2 and ω_3. These are the basic equations describing nonlinear parametric interactions [4]. We notice that they are coupled to each other via the nonlinear constant d.

8.3 OPTICAL SECOND-HARMONIC GENERATION

The first experiment in nonlinear optics [5] consisted of generating the second harmonic ($\lambda = 0.3470\ \mu$m) of a ruby laser beam ($\lambda = 0.694\ \mu$m) that was focused on a quartz crystal. The experimental arrangement is depicted in Figure 8-7. The conversion efficiency of this first experiment ($\sim 10^{-8}$) was improved by methods to be described below to a point where about 30 percent conversion has been observed in a single pass through a few centimeters length of a nonlinear crystal. This technique is finding important applications in generating short-wave radiation from longer-wave lasers.

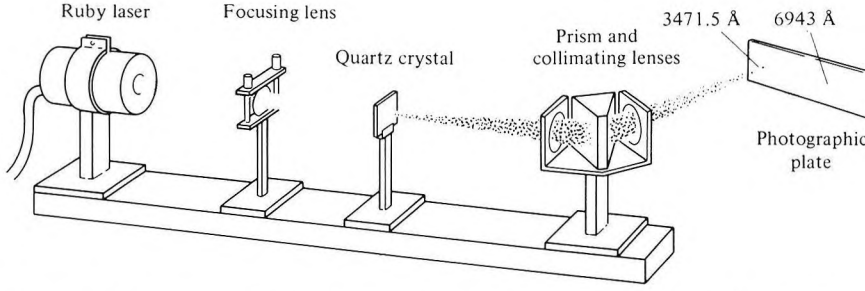

Figure 8-7 Arrangement used in first experimental demonstration of second-harmonic generation [5]. Ruby laser beam at $\lambda_0 = 0.694\ \mu$m is focused on a quartz crystal, causing generation of a (weak) beam at $\lambda_0/2 = 0.347\ \mu$m. The two beams are then separated by a prism and detected on a photographic plate.

In the case of second-harmonic generation, two of the three fields that figure in (8.2-13) are of the same frequency. We may thus put $\omega_1 = \omega_2 = \omega$, for which case the first two equations are the complex conjugate of one another and we need to consider only one of them. We take the input field at ω to correspond to E_1 in (8.2-13) and the second-harmonic field to E_3, and we put $\omega_3 = \omega_1 + \omega_2 = 2\omega$, neglecting the absorption, so $\sigma_{1,2,3} = 0$. The last equation becomes

$$\frac{dE^{(2\omega)}}{dz} = -i\omega \sqrt{\frac{\mu}{\epsilon}}\, d[E^{(\omega)}(z)]^2 e^{i(\Delta k)z} \tag{8.3-1}$$

where

$$\Delta k \equiv k_3 - 2k_1 = k^{(2\omega)} - 2k^{(\omega)} \tag{8.3-2}$$

To simplify the analysis further, we may assume that the depletion of the input wave at ω due to conversion of its power to 2ω is negligible. Under those conditions, which apply in the majority of the experimental situations, we can take $E^{(\omega)}(z) =$ constant in (8.3-1) and neglect its dependence on z. Assuming no input at 2ω—that is, $E^{(2\omega)}(0) = 0$—we obtain from (8.3-1) by integration the output field at the end of a crystal of length l:

$$E^{(2\omega)}(l) = -i\omega \sqrt{\frac{\mu}{\epsilon}}\, d[E^{(\omega)}]^2 \frac{e^{i\Delta kl} - 1}{i\Delta k}$$

The output intensity is proportional to

$$E^{(2\omega)}(l)E^{(2\omega)*}(l) = \left(\frac{\mu}{\epsilon_0}\right) \frac{\omega^2 d^2}{n^2} [E^{(\omega)}]^4 l^2 \frac{\sin^2(\Delta kl/2)}{(\Delta kl/2)^2} \tag{8.3-3}$$

Here we used $\epsilon/\epsilon_0 = n^2$, where n is the index of refraction. If the input beam is confined to a cross section $A(m^2)$, then, according to (1.3-26), the power per unit area (intensity) is related to the field by

$$I \equiv \frac{P_{2\omega}}{A} = \frac{1}{2}\sqrt{\frac{\epsilon}{\mu}}\,|E^{(2\omega)}|^2 \tag{8.3-4}$$

and (8.3-3) can be written as

$$\eta_{\mathrm{SHG}} \equiv \frac{P_{2\omega}}{P_\omega} = 2\left(\frac{\mu}{\epsilon_0}\right)^{3/2}\frac{\omega^2 d^2 l^2}{n^3}\frac{\sin^2(\Delta kl/2)}{(\Delta kl/2)^2}\frac{P_\omega}{A} \tag{8.3-5}$$

for the conversion efficiency from ω to 2ω. We notice that the conversion efficiency is proportional to the intensity P_ω/A of the fundamental beam.

Phase-Matching in Second-Harmonic Generation

According to (8.3-5), a prerequisite for efficient second-harmonic generation is that $\Delta k = 0$—or, using (8.3-2),

$$k^{(2\omega)} = 2k^{(\omega)} \tag{8.3-6}$$

If $\Delta k \neq 0$, the second-harmonic power generated at some plane, say z_1, having propagated to some other plane (z_2), is not in phase with the second-harmonic wave generated at z_2. This results in the interference described by the factor

$$\frac{\sin^2(\Delta kl/2)}{(\Delta kl/2)^2}$$

in (8.3-5). Two adjacent peaks of this spatial interference pattern are separated by the so-called "coherence length"

$$l_c = \frac{2\pi}{\Delta k} = \frac{2\pi}{k^{(2\omega)} - 2k^{(\omega)}} \tag{8.3-7}$$

The coherence length l_c is thus a *measure* of the *maximum crystal length that is useful in producing the second-harmonic power.* Under ordinary circumstances it may be no larger than 10^{-2} cm. This is because the index of refraction n_ω normally increases with ω so Δk is given by

$$\Delta k = k^{(2\omega)} - 2k^{(\omega)} = \frac{2\omega}{c}[n^{2\omega} - n^{\omega}] \tag{8.3-8}$$

where we used the relation $k^{(\omega)} = \omega n^{\omega}/c$. The coherence length is thus

$$l_c = \frac{\pi c}{\omega[n^{2\omega} - n^{\omega}]} = \frac{\lambda}{2[n^{2\omega} - n^{\omega}]} \tag{8.3-9}$$

where λ is the free-space wavelength of the fundamental beam. If we take a typical value of $\lambda = 1$ μm and $n^{2\omega} - n^{\omega} \simeq 10^{-2}$, we get $l_c \simeq 50$ μm. If l_c were to increase from 100 μm to 2 cm, as an example, according to (8.3-5) the second-harmonic power would go up by a factor of 4×10^4.

The technique that is used widely (see [6, 7]) to satisfy the *phase-matching* requirement $\Delta k = 0$ takes advantage of the natural birefringence of anisotropic crystals, which was discussed in Section 1.4. Using the relation $k^{(\omega)} = \omega\sqrt{\mu\epsilon_0 n^\omega}$, (8.3-6) becomes

$$n^{2\omega} = n^\omega \tag{8.3-10}$$

so the indices of refraction at the fundamental and second-harmonic frequencies must be equal. In normally dispersive materials the index of the ordinary wave or the extraordinary wave along a given direction increases with ω, as can be seen from Table 8-2. This makes it impossible to satisfy (8.3-10) when both the ω and 2ω beams are of the same type—that is, when both are extraordinary or ordinary. We can, however, under certain circumstances, satisfy (8.3-10) by making the two waves be of a different type. To illustrate the point, consider the dependence of the index of refraction of the extraordinary wave in a uniaxial crystal on the angle θ between the propagation direction and the crystal optic (z) axis. It is given by (1.4-12) as

$$\frac{1}{n_e^2(\theta)} = \frac{\cos^2\theta}{n_o^2} + \frac{\sin^2\theta}{n_e^2} \tag{8.3-11}$$

Table 8-2 Index of Refraction Dispersion Data of KH_2PO_4 (After Reference [8].)

	Index	
Wavelength, μm	n_o (ordinary ray)	n_e (extraordinary ray)
0.2000	1.622630	1.563913
0.3000	1.545570	1.498153
0.4000	1.524481	1.480244
0.5000	1.514928	1.472486
0.6000	1.509274	1.468267
0.7000	1.505235	1.465601
0.8000	1.501924	1.463708
0.9000	1.498930	1.462234
1.0000	1.496044	1.460993
1.1000	1.493147	1.459884
1.2000	1.490169	1.458845
1.3000	1.487064	1.457838
1.4000	1.483803	1.456838
1.5000	1.480363	1.455829
1.6000	1.476729	1.454797
1.7000	1.472890	1.453735
1.8000	1.468834	1.452636
1.9000	1.464555	1.451495
2.0000	1.460044	1.450308

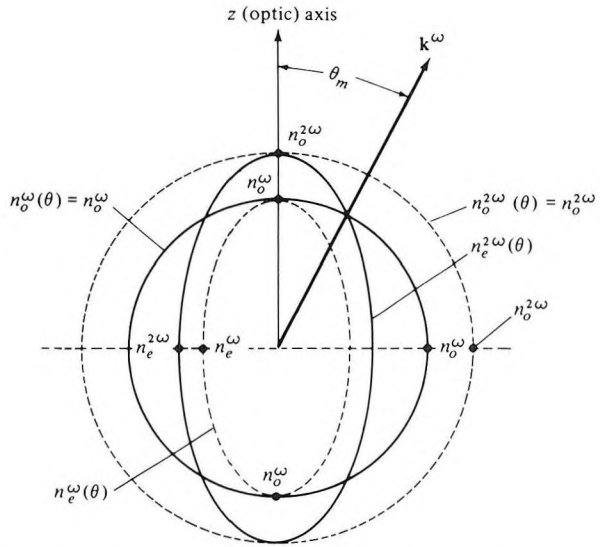

Figure 8-8 Normal (index) surfaces for the ordinary and extraordinary rays in a negative ($n_e < n_o$) uniaxial crystal. If $n_e^{2\omega} < n_o^{\omega}$, the condition $n_e^{2\omega}(\theta) = n_o^{\omega}$ is satisfied at $\theta = \theta_m$. The eccentricities shown are vastly exaggerated.

If $n_e^{2\omega} < n_o^{\omega}$, there exists an angle θ_m at which $n_e^{2\omega}(\theta_m) = n_o^{\omega}$; so if the fundamental beam (at ω) is launched along θ_m as an ordinary ray, the second-harmonic beam will be generated along the *same direction* as an extraordinary ray. The situation is illustrated by Figure 8-8. The angle θ_m is determined by the intersection between the sphere (shown as a circle in the figure) corresponding to the index surface of the ordinary beam at ω, and the index surface of the extraordinary ray $n_e^{2\omega}(\theta)$. The angle θ_m, which defines a cone, for negative uniaxial crystals—that is, crystals in which $n_e^{\omega} < n_o^{\omega}$—is that satisfying $n_e^{2\omega}(\theta_m) = n_o^{\omega}$ or, using (8.3-11),

$$\frac{\cos^2 \theta_m}{(n_o^{2\omega})^2} + \frac{\sin^2 \theta_m}{(n_e^{2\omega})^2} = \frac{1}{(n_o^{\omega})^2} \tag{8.3-12}$$

and, solving for θ_m,

$$\sin^2 \theta_m = \frac{(n_o^{\omega})^{-2} - (n_o^{2\omega})^{-2}}{(n_e^{2\omega})^{-2} - (n_o^{2\omega})^{-2}} \tag{8.3-13}$$

Numerical Example: Second-Harmonic Generation

Consider the problem of second-harmonic generation using the output of a pulsed ruby laser ($\lambda_0 = 0.6940\ \mu$m) in a KH_2PO_4 crystal (KDP) under the

following conditions:

$$l = 1 \text{ cm}$$
$$P_\omega/A = 10^8 \text{ W/cm}^2$$

The appropriate d coefficient is, according to Table 8-1, $d = d_{312} \cos\theta_m \times 2.5 \times 10^{-24}$ MKS units. Using these data in (8.3-5) and assuming $\Delta k = 0$ gives a conversion efficiency of

$$\frac{P_{(\lambda_0=0.347\ \mu\text{m})}}{P_{(\lambda_0=0.694\ \mu\text{m})}} \simeq 15 \text{ percent}$$

The angle θ_m between the z axis and the direction of propagation for which $\Delta k = 0$ is given by (8.3-13). The appropriate indices are taken from Table 8-2, and are

$$n_e(\lambda = 0.694\ \mu\text{m}) = 1.466 \qquad n_e(\lambda = 0.347\ \mu\text{m}) = 1.490$$
$$n_o(\lambda = 0.694\ \mu\text{m}) = 1.506 \qquad n_o(\lambda = 0.347\ \mu\text{m}) = 1.534$$

Substituting the foregoing data into (8.3-13) gives

$$\theta_m = 52°$$

To obtain phase-matching along this direction, the fundamental beam in the crystal must be polarized as appropriate to an ordinary ray in accordance with the discussion following (8.3-11).

We conclude from this example that very large intensities are needed to obtain high-efficiency second-harmonic generation. This efficiency will, according to (8.3-5), increase as the square of the nonlinear optical coefficient d and will consequently improve as new materials are developed. Another approach is to take advantage of the dependence of η_{SHG} on P_ω/A and to place the nonlinear crystal inside the laser resonator where the energy flux P_ω/A can be made very large.[4] This approach has been used successfully [10] and it will be discussed in considerable detail further in this chapter.

Experimental Verification of Phase-Matching

According to (8.3-5), if the phase-matching condition $\Delta k = 0$ is violated, the output power is reduced by a factor

$$F = \frac{\sin^2(\Delta kl/2)}{(\Delta kl/2)^2} \tag{8.3-14}$$

from its (maximum) phase-matched value. The phase mismatch $\Delta kl/2$ is

[4]The one-way power flow inside the optical resonator P_i is related to the power output P_e as $P_i = P_e/(1 - R)$, where R is the reflectivity.

given, according to (8.3-8), by

$$\frac{\Delta kl}{2} = \frac{\omega l}{c}\,[n_e^{2\omega}(\theta) - n_o^{\omega}] \tag{8.3-15}$$

and is thus a function of θ. If we use (8.3-11) to expand $n_e^{2\omega}(\theta)$ as a Taylor series near $\theta \simeq \theta_m$, retain the first two terms only, and assume perfect phase-matching at $\theta = \theta_m$ so $n_e^{2\omega}(\theta_m) = n_o^{\omega}$, we obtain

$$\begin{aligned}\Delta k(\theta)l &= -\frac{2\omega l}{c}\sin(2\theta_m)\,\frac{(n_e^{2\omega})^{-2} - (n_o^{2\omega})^{-2}}{2(n_o^{\omega})^{-3}}\,(\theta - \theta_m) \\ &\equiv 2\beta(\theta - \theta_m)\end{aligned} \tag{8.3-16}$$

where β, as defined by (8.3-16), is a constant depending on $n_e^{2\omega}$, $n_o^{2\omega}$, n_o^{ω}, ω, and l. If we plot the output power at 2ω as a function of θ we would expect, according to (8.3-5) and (8.3-16), to find it varying as

$$P_{2\omega}(\theta) \propto \frac{\sin^2[\beta(\theta - \theta_m)]}{[\beta(\theta - \theta_m)]^2} \tag{8.3-17}$$

Figure 8-9 shows an experimental plot of $P_{2\omega}(\theta)$ as well as a plot of (8.3-17).

Another phase-matching technique involves the introduction of an artificial spatial periodicity $\Delta l = 2\pi/\Delta k$ into the beams' path. This method is discussed in Problem 8.10 and the references quoted therein.

Second-Harmonic Generation with Focused Gaussian Beams

The analysis of second-harmonic generation leading to (8.3-5) is based on a plane wave model. In practice one uses Gaussian beams that are focused so as to reach their minimum radius (waist) inside the crystal. A typical situation is depicted in Figure 8-10. The incident Gaussian beam is characterized by confocal parameter z_0, which according to (2.5-11) is the dis-

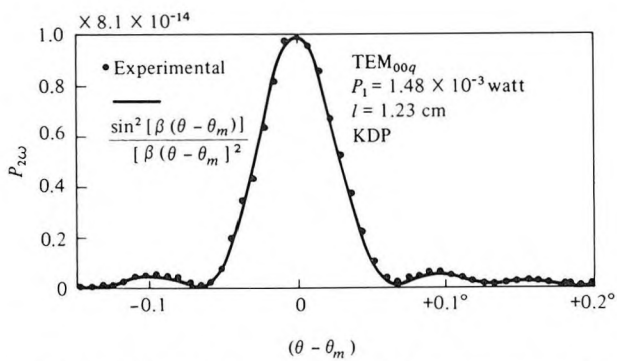

Figure 8–9 Variation of the second-harmonic power $P_{2\omega}$ with the angular departure $(\theta - \theta_m)$ from the phase-matching angle. (After Reference [11].)

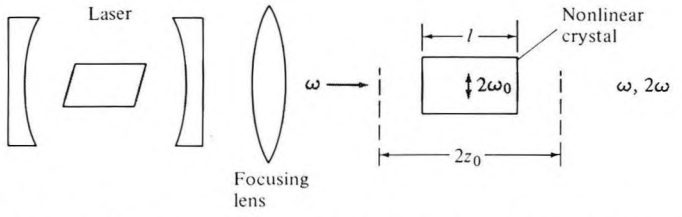

Figure 8–10 Second-harmonic generation with a focused Gaussian beam.

tance from the beam waist in which the beam "area" $\pi\omega^2$ is double that of the waist. We recall that $z_0 = \pi\omega_0^2 n/\lambda$, where ω_0 is the minimum beam radius (waist). If $z_0 \gg l$ (l is the crystal length), the beam area, hence the intensity, of the incident wave is nearly independent of z within the crystal, and we may apply the plane wave result (8.3-3) to write

$$|E^{(2\omega)}(r)|^2 = \frac{\mu}{\epsilon}\,\omega^2 d^2 |E^{(\omega)}(r)|^4 l^2\,\frac{\sin^2(\Delta kl/2)}{(\Delta kl/2)^2} \tag{8.3-18}$$

where $E^{(\omega)}(r)$ is taken as

$$E^{(\omega)}(r) \cong E_0 e^{-r^2/\omega_0^2} \tag{8.3-19}$$

as appropriate to a fundamental Gaussian beam. Using

$$P^{(\omega)} = \frac{1}{2}\sqrt{\frac{\epsilon}{\mu}}\int_{\text{cross section}} |E^{(\omega)}|^2\,dx\,dy \cong \sqrt{\frac{\epsilon}{\mu}}\,E_0^2\left(\frac{\pi\omega_0^2}{4}\right)$$

as well as (8.3-19), we obtain, by integrating (8.3-18),

$$\frac{P^{(2\omega)}}{P^{(\omega)}} = 2\left(\frac{\mu}{\epsilon_0}\right)^{3/2}\frac{\omega^2 d^2 l^2}{n^3}\left(\frac{P^{(\omega)}}{\pi\omega_0^2}\right)\frac{\sin^2(\Delta kl/2)}{(\Delta kl/2)^2} \tag{8.3-20}$$

where we used $(n^\omega)^2 n^{2\omega} \equiv n^3$.

Equation (8.3-20) is identical to (8.3-5). We must recall, however, that it was derived for a Gaussian beam input with $z_0 \gg l$. According to (8.3-20) in a crystal of length l and with a given input $P^{(\omega)}$, the output power $P^{(2\omega)}$ can be increased by decreasing ω_0. This is indeed the case until $z_0 (= \pi\omega_0^2 n/\lambda)$ becomes comparable to l. Further reduction of ω_0 (and z_0) will lead to a situation in which the beam begins to spread appreciably within the crystal, thus leading to a reduced intensity and a reduced second-harmonic generation. It is thus reasonable to focus the beam until $l = 2z_0$. At this point $\omega_0^2 = \lambda l/2\pi n$, which is referred to as confocal focusing, and (8.3-20) becomes

$$\eta \equiv \left.\frac{P^{(2\omega)}}{P^{(\omega)}}\right|_{\text{confocal focusing}} = \frac{2}{\pi c}\left(\frac{\mu}{\epsilon_0}\right)^{3/2}\frac{\omega^3 d^2 l}{n^2}\,P^{(\omega)}\,\frac{\sin^2(\Delta kl/2)}{(\Delta kl/2)^2} \tag{8.3-21}$$

A more exact analysis of second-harmonic generation with focused Gaussian beam shows that the maximum conversion efficiency is approximately 20 percent higher than the confocal result (8.3-21).

The main difference between (8.3-21) and the plane wave result (8.3-5) is that the conversion efficiency in this case increases as l instead of l^2. This reflects the fact that a longer crystal entails the use of a larger beam spot size ω_0 so as to keep $z_0 \approx l/2$, which reduces the intensity of the fundamental beam.

Example: Optimum Focusing

Consider second harmonic conversion under confocal focusing conditions, in KH_2PO_4 from $\lambda = 1\ \mu$m to $\lambda = 0.5\ \mu$m. Using $l = 1$ cm, $d_{\text{eff}} = 3.6 \times 10^{-24}$ MKS, $n = 1.5$, we obtain from (8.3-21)

$$\frac{P^{(2\omega)}}{P^{(\omega)}} = 4.4 \times 10^{-6}\, P^{(\omega)}$$

Second-Harmonic Generation with a Depleted Input

The expression (8.3-5) for the conversion efficiency in second harmonic generation was derived assuming negligible depletion of the fundamental beam at ω. It is, therefore, valid only for cases where the conversion efficiency is small, i.e., $\eta_{\text{SHG}} \ll 1$. A study of Equation (8.2-13) or the intuitive understanding of parametric processes which the student may have acquired by now shows that, assuming phase matching and a sufficiently long crystal, the conversion process $\omega \rightarrow 2\omega$ continues with distance and that it is not unreasonable to expect conversion efficiencies approaching unity. To consider this possibility, we return to Equation (8.2-13), but this time, anticipating pump depletion, the fundamental beams $E_1(z)$ and $E_2(z)$ are allowed to depend on z. We transform to a new set of field variables A_l defined by[5]

$$A_l \equiv \sqrt{\frac{n_l}{\omega_l}}\, E_l \qquad l = 1, 2, 3 \tag{8.3-22}$$

where $n_l^2 = \epsilon_l/\epsilon_0$, i.e., n_l is the index of refraction of wave l. See discussion following Equation (8.6-17) to better appreciate the transformation (8.3-22). The result is

$$\begin{aligned}
\frac{dA_1}{dz} &= -\frac{\alpha_1}{2} A_1 - \frac{i}{2} \kappa A_2^* A_3 e^{-i(\Delta k)z} \\
\frac{dA_2^*}{dz} &= -\frac{\alpha_2}{2} A_2^* + \frac{i}{2} \kappa A_1 A_3^* e^{i(\Delta k)z} \\
\frac{dA_3}{dz} &= -\frac{\alpha_3}{2} A_3 - \frac{i}{2} \kappa A_1 A_2 e^{i(\Delta k)z}
\end{aligned} \tag{8.3-23}$$

[5]It follows from (8.3-22) that $|A_l|^2$ is proportional to the photon density at ω_l [see Equation (8.6-17)].

where

$$\alpha_l \equiv \sigma_l \sqrt{\frac{\mu}{\epsilon_l}}$$

$$\kappa \equiv d \sqrt{\left(\frac{\mu}{\epsilon_0}\right) \frac{\omega_1 \omega_2 \omega_3}{n_1 n_2 n_3}}$$

$$\Delta k \equiv k_3 - (k_1 + k_2) \tag{8.3-24}$$

In the case of second-harmonic generation, $A_1 = A_2$ and (8.3-23) become

$$\frac{dA_1}{dz} = -i \frac{\kappa}{2} A_3 A_1^*$$

$$\frac{dA_3}{dz} = -i \frac{\kappa}{2} A_1^2 \tag{8.3-25}$$

where we assumed transparent ($\alpha_l = 0$) media and phase matching ($\Delta k = 0$). It follows from (8.3-25) that if we choose, without loss of generality, $A_1(0)$ as a real number, then $A_1(z)$ is real and (8.3-25) can be rewritten in the form

$$\frac{dA_1}{dz} = -\frac{1}{2} \kappa A_3' A_1$$

$$\frac{dA_3'}{dz} = \frac{1}{2} \kappa A_1^2 \tag{8.3-26}$$

where $A_3 \equiv -iA_3'$. It follows from (8.3-26) that

$$\frac{d}{dz}(A_1^2 + A_3'^2) = 0$$

(i.e., for each photon "removed" from beam 1, one photon is added to beam 3; energy is conserved, since a photon is also removed simultaneously from beam 2).

Assuming no input at ω_3, we have $A_1^2 + A_3'^2 = A_1^2(0)$, and the second of (8.3-26) becomes

$$\frac{dA_3'}{dz} = \frac{1}{2} \kappa (A_1^2(0) - A_3'^2)$$

leading to a solution

$$A_3'(z) = A_1(0) \tanh[\tfrac{1}{2} \kappa A_1(0) z] \tag{8.3-27}$$

We note that as $\kappa A_1(0) z \to \infty$, $A_3'(z) \to A_1(0)$ so that all the input photons at ω are converted into half (since $A_1 = A_2$) as many photons at 2ω and the power conversion efficiency approaches unity. In the general case

$$\eta_{\text{SHG}} \equiv \frac{P^{(2\omega)}}{P^{(\omega)}} = \frac{|A_3(z)|^2}{|A_1(0)|^2} = \tanh^2[\tfrac{1}{2} \kappa A_1(0) z] \tag{8.3-28}$$

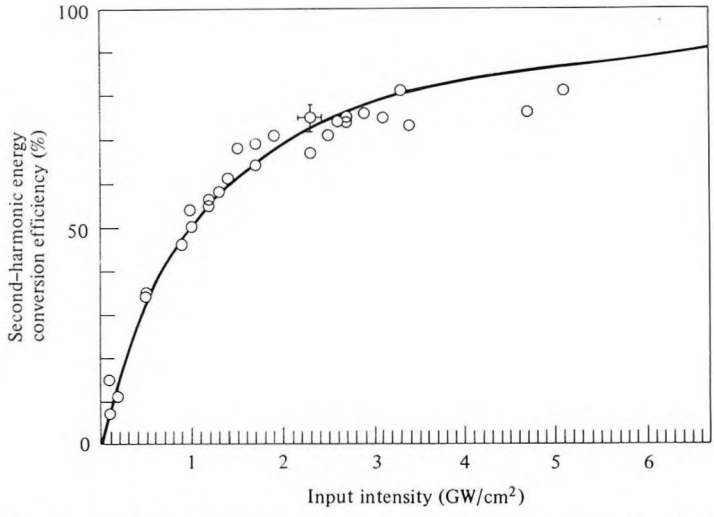

Figure 8-11 Frequency doubling energy conversion efficiency. Solid curve: theoretical prediction of Equation (8.3-28) (recall that $A_1(0) \propto \sqrt{I_{in}}$). The circles correspond to experimental points. (After supplementary Reference [30].)

A plot of the theoretically predicted relation (8.3-28) as well as of experimental data obtained in converting from $\lambda = 1.06$ to $\lambda = 0.53$ μm is shown in Figure 8-11.

8.4 SECOND-HARMONIC GENERATION INSIDE THE LASER RESONATOR

According to the numerical example of Section 8.3 and Figure 8-11 we need to use large power densities at the fundamental frequency ω to obtain appreciable conversion from ω to 2ω in typical nonlinear optical crystals. These power densities are not usually available from continuous (CW) lasers. The situation is altered, however, if the nonlinear crystal is placed within the laser resonator. The intensity (one-way power per unit area in watts per square meter) inside the resonator exceeds its value outside a mirror by $(1 - R)^{-1}$, where R is the mirror reflectivity. If $R \simeq 1$, the enhancement is very large and since the second-harmonic conversion efficiency is, according to (8.3-5), proportional to the intensity, we may expect a far more efficient conversion inside the resonator. We will show below that under the proper conditions we can extract the *total available power* of the laser at 2ω instead of at ω and in that sense obtain 100 percent conversion efficiency. In order to appreciate the last statement, consider as an example the case of a (CW) laser in which the maximum power output, at a given pumping rate, is available when the output mirror has a (optimal) transmission of 5 percent.

The output mirror is next replaced with one having 100 percent reflection at ω and a nonlinear crystal is placed inside the laser resonator. If with the crystal inside the conversion efficiency from ω to 2ω in a *single pass* is 5 percent, the laser is loaded optimally as in the previous case except that the coupling is attributable to loss of power caused by second-harmonic generation instead of by the output mirror. It follows that the power generated at 2ω is the same as that coupled previously through the mirror and that the total available power of a laser can thus be converted to the second harmonic.

An experimental setup similar to the one used in the first internal second-harmonic generation experiment [10] is shown in Figure 8-12. The Nd^{3+}:YAG laser (see Chapter 7 for a description of this laser) emits a (fundamental) wave at $\lambda_0 = 1.06\ \mu m$. The mirrors are, as nearly as possible, totally reflecting at $\lambda_0 = 1.06\ \mu m$. A $Ba_2NaNb_5O_{15}$ crystal is used to generate the second harmonic at $\lambda_0 = 0.53\ \mu m$. The latter is coupled through the mirror—which, ideally, transmits all the radiation at this wavelength.

In the mathematical treatment of internal second-harmonic generation that follows we use the results of the analysis of optimum power coupling in laser oscillators of Section 6.5.

The mirror transmission T_{opt} that results in the maximum power output from a laser oscillator is given by (6.5-11) as

$$T_{opt} = \sqrt{g_0 L_i} - L_i \tag{8.4-1}$$

where L_i is the residual (that is, unavoidable) fractional intensity loss per pass and g_0 is the fractional unsaturated gain per pass.[6] The useful power output under optimum coupling is, according to (6.5-12),

$$P_o = I_s A(\sqrt{g_0} - \sqrt{L_i})^2 \tag{8.4-2}$$

where the saturation intensity of the laser transition $I_s A$ was given by (5.6-9)

[6]We may recall here that the residual losses include all loss mechanisms except those representing useful power coupling. The unsaturated gain g_0 is that exercised by a very weak wave and represents the maximum available gain at a given pumping strength.

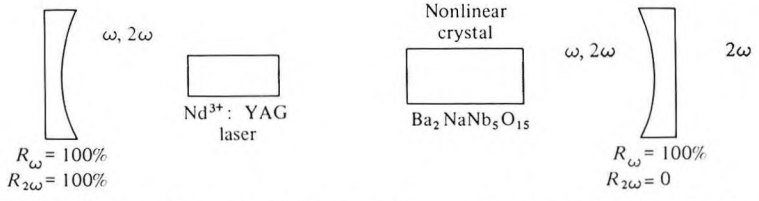

Figure 8-12 Typical setup for second-harmonic conversion inside a laser resonator. (After Reference [9].)

as[7]

$$I_s = \frac{8\pi n^2 h\nu \Delta \nu}{\lambda^2 (t_2/t_{\text{spont}})} \tag{8.4-3}$$

In the present problem the conversion from ω to 2ω can be considered, as far as the ω oscillation is concerned, just as another loss mechanism. We may think of it as due to a mirror with a transmission T' taken as equal to the conversion efficiency (from ω to 2ω) per pass, which, according to (8.3-5), is

$$T' \equiv \frac{P_{2\omega}}{P_\omega} = 2\left(\frac{\mu_0}{\epsilon_0}\right)^{3/2} \frac{\omega^2 d^2 l^2}{n^3} \left[\frac{\sin^2(\Delta k l/2)}{(\Delta k l/2)^2}\right] \frac{P_\omega}{A} \tag{8.4-4}$$

where d is the crystal nonlinear coefficient, l its length, A its cross-sectional area, Δk the wave-vector mismatch, and P_ω the one-way traveling power *inside* the laser. We can rewrite T' in the form

$$T' = \kappa P_\omega \tag{8.4-5}$$

where the value of the constant κ is evident from Equation (8.4-4). The equivalent mirror transmission T' is thus proportional to the power.

Using the last result in (8.4-1), we find immediately that at optimum conversion the product κP_ω must have the value

$$(\kappa P_\omega)_{\text{opt}} = \sqrt{g_0 L_i} - L_i \tag{8.4-6}$$

The total loss per pass seen by the fundamental beam is the sum of the conversion loss (κP_ω) and the residual losses, which, under optimum coupling, becomes

$$L_{\text{opt}} = L_i + (\kappa P_\omega)_{\text{opt}} = \sqrt{g_0 L_i} \tag{8.4-7}$$

Our next problem is to find the internal power P_ω at optimum coupling so that using (8.4-4) we may calculate the second-harmonic power. We start with the expression (6.5-6) for the total power P_e extracted from the laser atoms and replace the loss L by its optimum value (8.4-7) to obtain

$$\begin{aligned}(P_e)_{\text{opt}} &= P_s\left(\frac{g_0}{L_{\text{opt}}} - 1\right) = P_s\left(\sqrt{\frac{g_0}{L_i}} - 1\right) \\ &= \frac{8\pi n^3 h \Delta \nu V}{\lambda^3 (t_c)_{\text{opt}}} \left(\frac{t_{\text{spont}}}{t_2}\right)\left(\sqrt{\frac{g_0}{L_i}} - 1\right) = L_{\text{opt}} I_s A \left(\sqrt{\frac{g_0}{L_i}} - 1\right)\end{aligned} \tag{8.4-8}$$

---

[7] I_s is, according to (5.6-8) [and putting $g(\nu)^{-1} = \Delta\nu$], the optical intensity (watts per square meter) that reduces the inversion, hence the gain, to one-half its zero intensity (unsaturated) value.

where to get the last equality we used relation (4.7-2)

$$t_c = \frac{nl}{cL}$$

to relate the resonator decay time t_c to the loss per pass L. The fraction of the total power P_e emitted by the atoms that is available as useful output is T'/L. This power is also given by the product $P_\omega T'$ of the one-way internal power P_ω and the fraction T' of this power that is converted per pass. Equating these two forms gives

$$P_\omega = \frac{P_e}{L}$$

and using (8.4-8) we get

$$(P_\omega)_{\text{opt}} = I_s A\left(\sqrt{\frac{g_0}{L_i}} - 1\right) \tag{8.4-9}$$

for the one-way fundamental power inside the laser under optimum coupling conditions. The amount of second-harmonic power generated under optimum coupling is

$$(P_{2\omega})_{\text{opt}} = (\kappa P_\omega)_{\text{opt}}(P_\omega)_{\text{opt}}$$

which, through the use of (8.4-6) and (8.4-9), results in

$$(P_{2\omega})_{\text{opt}} = I_s A(\sqrt{g_0} - \sqrt{L_i})^2 \tag{8.4-10}$$

This is the same expression as the one previously obtained in (6.5-12) for the maximum available power output from a laser oscillator.

The nonlinear coupling constant κ was defined by (8.4-4) and (8.4-5) as

$$\kappa = 2\left(\frac{\mu_0}{\epsilon_0}\right)^{3/2} \frac{\omega^2 d^2 l^2}{n^3 A}\left(\frac{\sin^2(\Delta kl/2)}{(\Delta kl/2)^2}\right) \tag{8.4-11}$$

Its value under optimum coupling can be derived from (8.4-6) and (8.4-9) and is

$$\kappa_{\text{opt}} = \frac{(\kappa P_\omega)_{\text{opt}}}{(P_\omega)_{\text{opt}}} = \frac{L_i}{I_s A} \tag{8.4-12}$$

and is thus *independent of the pumping strength*.[8] It follows that once κ is adjusted to its optimum value $L_i/I_s A$, it remains optimal at any pumping level. This is quite different from the case of optimum coupling in ordinary lasers, in which optimum mirror transmission was found [see (6.5-11)] to depend on the pumping strength.

---

[8]We recall here that the pumping strength in our analysis is represented by the unsaturated gain g_0.

In closing we may note that apart from its dependence on the crystal length l, the nonlinear coefficient d, and the beam cross section A, κ depends also on the phase mismatch Δkl. Since Δk was shown in (8.3-15) to depend on the direction of propagation in the crystal, we can use the crystal orientation as a means of varying κ.

Numerical Example: Internal Second-Harmonic Generation

Consider the problem of designing an internal second harmonic generator of the type illustrated in Figure 8-12. The Nd^{3+}:YAG laser is assumed to have the following characteristics:

$\lambda_0 = 1.06\ \mu m = 1.06 \times 10^{-6}$ meter

$\Delta\nu = 1.35 \times 10^{11}$ Hz (width of the spectral gain profile)

Beam diameter (averaged over entire resonator length) = 2 mm

L_i = internal loss per pass = 2×10^{-2}

$n = 1.5$

The crystal used for second-harmonic generation is $Ba_2NaNb_5O_{15}$, whose second-harmonic coefficient (see Table 8-1) is $d \simeq 1.1 \times 10^{-22}$ MKS units.

Our problem is to calculate the length l of the nonlinear crystal that results in a full conversion of the optimally available fundamental power into the second harmonic at $\lambda = 0.53\ \mu m$. The crystal is assumed to be oriented at the phase-matching angle, so $\Delta k = k^{2\omega} - 2k^{\omega} = 0$.

The optimum coupling parameter is given by (8.4-12) as $\kappa_{opt} = L_i/I_sA$, where I_s is the saturation intensity defined by (8.4-3). Using the foregoing data in (8.4-3) gives

$$I_sA = 2 \text{ watts}$$

which, taking $L_i = 2 \times 10^{-2}$, yields

$$\kappa_{opt} = 10^{-2}$$

Next we use the definition (8.4-11)

$$\kappa = 2\left(\frac{\mu_0}{\epsilon_0}\right)^{3/2} \frac{\omega^2 d^2 l^2}{n^3 A}$$

where we put $\Delta k = 0$ and take the beam diameter at the crystal as 50 μm. (The crystal can be placed near a beam waist so the diameter is a minimum.) Equating the last expression to $\kappa_{opt} = 10^{-2}$ using the numerical data given above, and solving for the crystal length, results in

$$l_{opt} = 0.804 \text{ cm}$$

8.5 PHOTON MODEL OF SECOND-HARMONIC GENERATION

A very useful point of view and one that follows directly from the quantum mechanical analysis of nonlinear optical processes [12] is based on the photon model illustrated in Figure 8-13. According to this picture, the basic process of second-harmonic generation can be viewed as an annihilation of two photons at ω and a simultaneous creation of a photon at 2ω. Recalling that a photon has an energy $\hbar\omega$ and a momentum $\hbar\mathbf{k}$, it follows that if the fundamental conversion process is to conserve momentum as well as energy that

$$\mathbf{k}^{(2\omega)} = 2\mathbf{k}^{(\omega)} \tag{8.5-1}$$

which is a generalization to three dimensions of the condition $\Delta k = 0$ shown in Section 8.3 to lead to maximum second-harmonic generation.

8.6 PARAMETRIC AMPLIFICATION

Optical parametric amplification in its simplest form involves the transfer of power from a "pump" wave at ω_3 to waves at frequencies ω_1 and ω_2, where $\omega_3 = \omega_1 + \omega_2$. It is fundamentally similar to the case of second-harmonic generation treated in Section 8.3. The only difference is in the direction of power flow. In second-harmonic generation, power is fed from the low-frequency optical field at ω to the field at 2ω. In parametric amplification, power flow is from the high-frequency field (ω_3) to the low-frequency fields

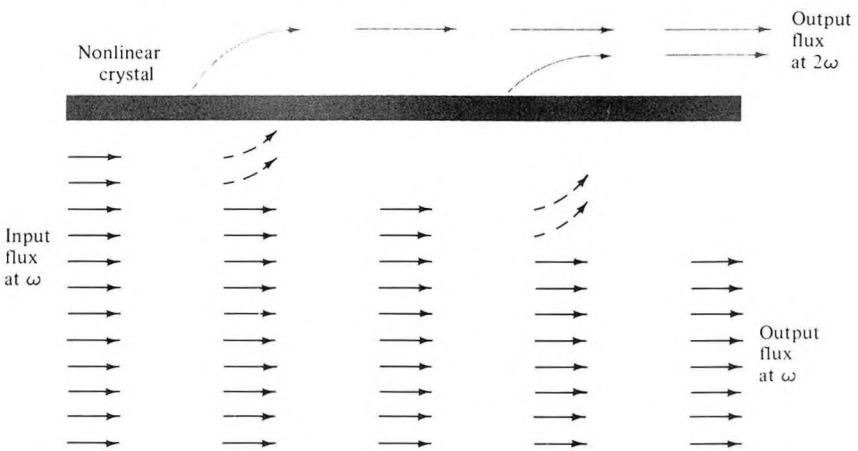

Figure 8-13 Schematic representation of the process of second-harmonic generation. Input photons (each arrow represents one photon) at ω are "annihilated" by the nonlinear crystal in pairs, with a new photon at 2ω being created for each annihilated pair. (Note that in reality both ω and 2ω occupy the same space inside the crystal.)

at ω_1 and ω_2. In the special case where $\omega_1 = \omega_2$, we have the exact reverse of second-harmonic generation. This is the case of the so-called degenerate parametric amplification.

Before we embark on a detailed analysis of the optical case it may be worthwhile to review some of the low-frequency beginnings of parametric oscillation.

Consider a classical nondriven oscillator whose equation of motion is given by

$$\frac{d^2v}{dt^2} + \kappa \frac{dv}{dt} + \omega_0^2 v = 0 \tag{8.6-1}$$

The variable v may correspond to the excursion of a mass M, which is connected to a spring with a constant $\omega_0^2 M$, or to the voltage across a parallel RLC circuit, in which case $\omega_0^2 = (LC)^{-1}$ and $\kappa = (RC)^{-1}$. The solution of (8.6-1) is

$$v(t) = v(0) \exp\left(-\frac{\kappa t}{2}\right) \exp\left(\pm i \sqrt{\omega_0^2 - \frac{\kappa^2}{4}}\, t\right) \tag{8.6-2}$$

that is, a damped sinusoid.

In 1883 Lord Rayleigh [13], investigating parasitic resonances in pipe organs, considered the consequences of the following equation

$$\frac{d^2v}{dt^2} + \kappa \frac{dv}{dt} + (\omega_0^2 + 2\alpha \sin \omega_p t)v = 0 \tag{8.6-3}$$

This equation may describe an oscillator in which an energy storage parameter (mass or spring constant in the mechanical oscillator, L or C in the RLC oscillator) is modulated at a frequency ω_p. As an example consider the case of the RLC circuit shown in Figure 8-14, in which the capacitance is modulated according to

$$C = C_0\left(1 - \frac{\Delta C}{C_0} \sin \omega_p t\right) \tag{8.6-4}$$

The equation of the voltage across the RLC circuit is given by (8.6-1) with $\omega_0^2 = (LC)^{-1}$.

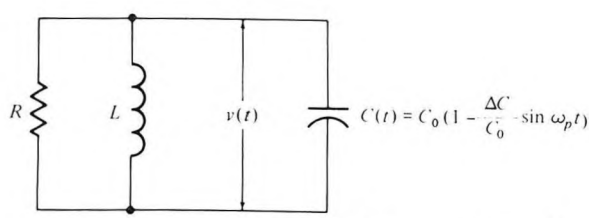

Figure 8-14 A degenerate parametric oscillator with a sinusoidally modulated capacitance.

Using (8.6-4) and assuming $\Delta C \ll C_0$, (8.6-1) becomes

$$\frac{d^2v}{dt^2} + \kappa \frac{dv}{dt} + \frac{1}{LC_0}\left(1 + \frac{\Delta C}{C_0} \sin \omega_p t\right) v = 0 \tag{8.6-5}$$

which, if we make the identification

$$\omega_0^2 = \frac{1}{LC_0}, \qquad \alpha = \frac{\omega_0^2 \Delta C}{2C_0} \tag{8.6-6}$$

is identical to (8.6-3).

The most important feature of the parametrically driven oscillator described by (8.6-3) is that it is capable of *sustained oscillation* at ω_0. To show this let us assume a solution

$$v = a \cos[\omega t + \phi] \tag{8.6-7}$$

Expanding sin $\omega_p t$ in (8.6-3) in terms of exponentials, substituting (8.6-7) and neglecting nonsynchronous terms oscillating at $(\omega_p + \omega)$ leads to

$$(\omega_0^2 - \omega^2)e^{i(\omega t+\phi)} + i\omega\kappa e^{i(\omega t+\phi)} - i\alpha e^{i[(\omega_p-\omega)t-\phi]} = 0 \tag{8.6-8}$$

From (8.6-8) it follows that steady-state oscillation is possible if

$$\omega_p = 2\omega \qquad (\text{so that } \omega_p - \omega = \omega)$$
$$\omega = \omega_0 \qquad \phi = 0 \text{ or } \pi \qquad \alpha = \omega\kappa \tag{8.6-9}$$

or, in words:

The pump frequency ω_p is twice the oscillation frequency ω_0. The oscillation phase[9] is $\phi = 0$ or π and the strength of the pumping α must satisfy $\alpha = \omega\kappa$. The last condition is referred to as the "start-oscillation condition" or "threshold condition," since it gives the pumping strength (α) needed to overcome the losses (κ) at the oscillation threshold. In the case of the *RLC* circuit, whose capacitance is modulated according to (8.6-4), the threshold oscillation condition $\alpha = \omega\kappa$ can be written with the aid of (8.6-6) as

$$\frac{\Delta C}{2C_0} = \frac{\kappa}{\omega_0} = \frac{1}{Q} \tag{8.6-10}$$

where the quality factor $Q = \omega_0 RC$ is related to the decay rate κ by $\kappa = \omega_0/Q$.

In practice, if the capacitance of the circuit shown in Figure 8-14 is modulated so that condition (8.6-10) is satisfied, the circuit will break into spontaneous oscillation at a frequency $\omega_0 = \omega_p/2$. This constitutes a transfer of energy from ω_p to $\omega_p/2$.

The physical nature of this transfer may become clearer if we consider the time behavior of the voltage $v(t)$, the charge $q(t)$, and the capacitance $C(t)$ as illustrated in Figure 8-15.

---

[9]The phase ϕ is of fundamental importance and it is defined relative to that of the pump oscillation as given by (8.6-4).

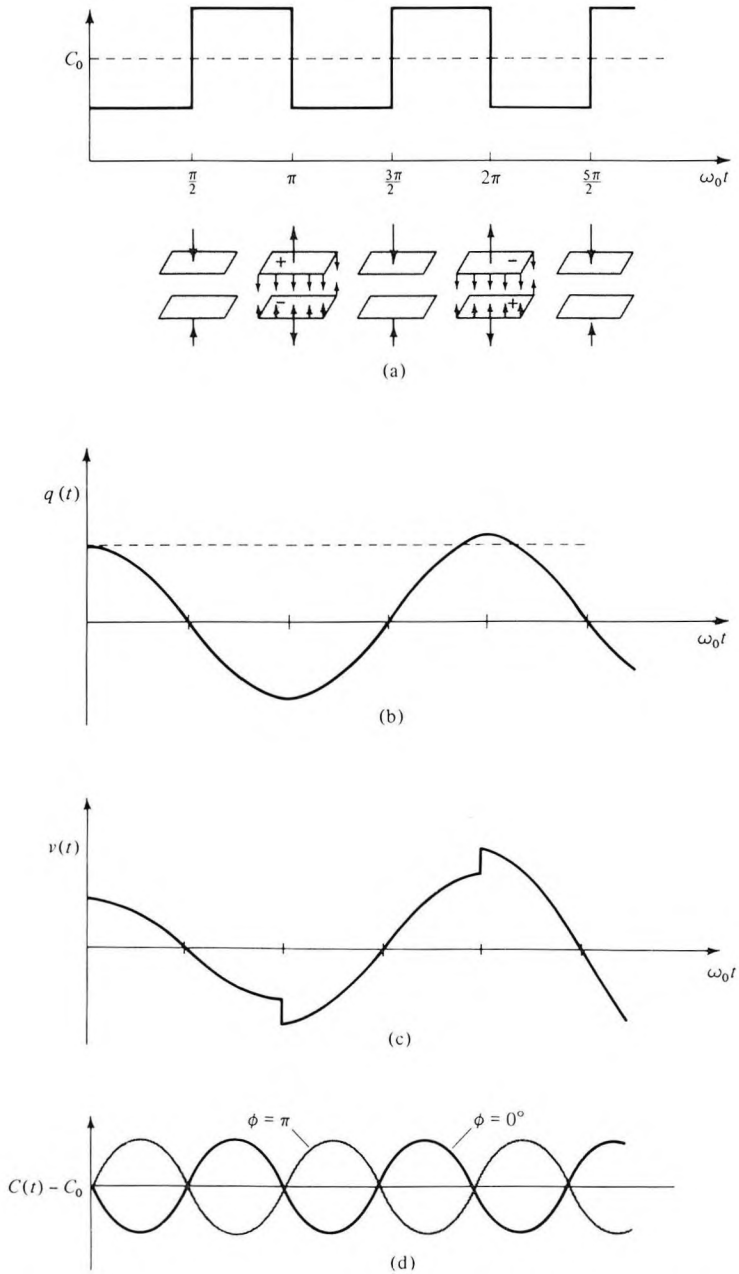

Figure 8-15 Physical model of a capacitively pumped parametric oscillator. (a) Square-wave capacitance variation at twice the circuit oscillation frequency. (Also shown is the motion of the capacitor plates, the charge, and the forces on the plates.) (b) The charge on one of the capacitor plates. (c) The voltage across the circuit. (d) Variation of the capacitance $C(t)$ at two phases relative to that of the charge.

$C(t)$ is a parallel-plate capacitor whose capacitance is periodically varied. Assume first that $C(t)$ is varied as in Figure 8-15(a) by pulling the capacitor plates apart and pushing them together again [$C \propto$ (plate separation)$^{-1}$]. At the same time the circuit is caused to oscillate so that the charge $q(t)$ on the capacitor plates varies as in Figure 8-15(b). Now, according to Figure 8-15(a), when the charge on the plates is a maximum, the plates are pulled apart slightly. The charge cannot change instantaneously, but since work must be done (against the Coulomb attraction of the opposite charges on the capacitor plates) to separate the plates, energy is fed into the capacitor and appears as a sudden increase in the voltage ($v = q/C$, $\mathcal{E} = \frac{1}{2}q^2/C$), as in Figure 8-15(c). One quarter of a period later, the charge and thus the field between the plates is zero and the plates can be returned to their original position with no energy expenditure. At the end of half a cycle, the charge has reversed sign and is again a maximum, so the plates are pulled apart once more. This process is then repeated many times, causing the total voltage to increase twice in each oscillation cycle. In this way, energy at *twice* the resonant frequency is pumped into the circuit where it appears as an increase in energy of the resonant frequency.

There are two noteworthy features to this degenerate oscillator. First, the frequency of the pump *must* be very nearly twice the resonant frequency of the oscillator for gain to occur, in agreement with the previous conclusions, see (8.6-9). In addition, the phase of the pump relative to the charge on the capacitor plates must be chosen properly. Consider the case where $C(t) = C_0 \pm \Delta C \sin 2\omega_0 t$, as in Figure 8-15(d). If we take the minus sign, which corresponds to the $\phi = 0°$ curve, then energy is continuously fed *into* the system as described above. If, however, the pumping phase is inverted (that is, the plus sign), then the capacitor plates are pushed together when the charge is a maximum, thus performing work, giving up energy, and decreasing the total voltage. Any initial oscillations that may be present will be damped out. The phase condition ($\phi = 0$) agrees with the second of (8.6-9).

To make a connection between the lumped-circuit parametric oscillator and the optical nonlinearity discussed in (8.1-14) we show that the (time) modulation of a capacitance at some frequency ω_p which was shown to give rise to oscillation at $\omega_p/2$ is formally equivalent to applying a field at ω_p to a nonlinear dielectric in which the polarization p and the electric field e are related by

$$p = \epsilon_0 \chi e + de^2 \tag{8.6-11}$$

This can be done by considering a parallel-plate capacitance of area A and separation s that is filled with a medium whose polarization is given by (8.6-11). Using the relations[10]

$$d(t) = \epsilon_0 e(t) + p(t) = \epsilon e(t) \tag{8.6-12}$$

[10]The electric displacement $d(t)$ should not be confused with the nonlinear constant d in (8.6-11).

the dielectric constant ϵ can be written as

$$\epsilon = \epsilon_0(1 + \chi) + de$$

and the capacitance $C = \epsilon A/s$ as

$$C = \frac{\epsilon_0(1 + \chi)A}{s} + \frac{Ad}{s} e \tag{8.6-13}$$

If the electric field is given by

$$e = -E_0 \sin \omega_p t$$

the capacitance becomes

$$C = \frac{\epsilon_0(1 + \chi)A}{s} - \frac{AdE_0}{s} \sin \omega_p t \tag{8.6-14}$$

which is of a form identical to (8.6-4). It follows that the two points of view used to describe parametric processes—the one represented by (8.6-4), in which an energy-storage parameter is modulated, and that in which the electric (or magnetic) response is nonlinear, as in (8.6-11)—are equivalent.

We return now to the basic nonlinear parametric equations (8.2-13) to analyze the case of optical parametric amplification. We find it convenient as in (8.3-22) to introduce a new field variable, defined by

$$A_l \equiv \sqrt{\frac{n_l}{\omega_l}} E_l \qquad l = 1, 2, 3 \tag{8.6-15}$$

so that the power flow per unit area at ω_l is given by

$$\frac{P_l}{A} = \frac{1}{2} \sqrt{\frac{\epsilon_0}{\mu}} n_l |E_l|^2 = \frac{1}{2} \sqrt{\frac{\epsilon_0}{\mu}} \omega_l |A_l|^2 \tag{8.6-16}$$

when n_l is the index of refraction at ω_l. The power flow P_l/A per unit area is related to the flux N_l (photons per square meter per second) by

$$\frac{P_l}{A} = N_l \hbar \omega_l = \frac{1}{2} \sqrt{\frac{\epsilon_0}{\mu}} |A_l|^2 \omega_l \tag{8.6-17}$$

so that $|A_l|^2$ is proportional to the photon flux at ω_l. The equations of motion (8.2-13) for the A_l variables become

$$\begin{aligned}
\frac{dA_1}{dz} &= -\frac{1}{2} \alpha_1 A_1 - \frac{i}{2} \lambda A_2^* A_3 e^{-i(\Delta k)z} \\
\frac{dA_2^*}{dz} &= -\frac{1}{2} \alpha_2 A_2^* + \frac{i}{2} \lambda A_1 A_3^* e^{i(\Delta k)z} \\
\frac{dA_3}{dz} &= -\frac{1}{2} \alpha_3 A_3 - \frac{i}{2} \lambda A_1 A_2 e^{i(\Delta k)z}
\end{aligned} \tag{8.6-18}$$

where

$$\Delta k \equiv k_3 - (k_1 + k_2)$$
$$\kappa \equiv d\sqrt{\left(\frac{\mu}{\epsilon_0}\right)\frac{\omega_1\omega_2\omega_3}{n_1n_2n_3}}$$
$$\alpha_l \equiv \sigma_l\sqrt{\frac{\mu}{\epsilon_l}} \qquad l = 1, 2, 3 \tag{8.6-19}$$

The advantage of using the A_l instead of E_l is now apparent since, unlike (8.2-13), relations (8.6-18) involve a single coupling parameter κ.

We will now use (8.6-18) to solve for the field variables $A_1(z)$, $A_2(z)$, and $A_3(z)$ for the case in which three waves with amplitudes $A_1(0)$, $A_2(0)$, and $A_3(0)$ at frequencies ω_1, ω_2, and ω_3, respectively, are incident on a nonlinear crystal at $z = 0$. We take $\omega_3 = \omega_1 + \omega_2$, $\alpha_1 = \alpha_2 = \alpha_3 = 0$ (no losses), and $\Delta k = k_3 - k_1 - k_2 = 0$. In addition, we assume that $\omega_1|A_1(z)|^2$ and $\omega_2|A_2(z)|^2$ remain small compared to $\omega_3|A_3(0)|^2$ throughout the interaction region. This last condition, in view of (8.6-17), is equivalent to assuming that the power drained off the "pump" (at ω_3) by the "signal" (ω_1) and idler (ω_2) is negligible compared to the input power at ω_3. This enables us to view $A_3(z)$ as a constant. With the assumptions stated above, equations (8.6-18) become

$$\frac{dA_1}{dz} = -\frac{ig}{2}A_2^* \qquad \frac{dA_2^*}{dz} = \frac{ig}{2}A_1 \tag{8.6-20}$$

where

$$g \equiv \kappa A_3(0) = \sqrt{\left(\frac{\mu}{\epsilon_0}\right)\frac{\omega_1\omega_2}{n_1n_2}}\,dE_3(0) \tag{8.6-21}$$

The solution of the coupled equations (8.6-20) subject to the initial conditions $A_1(z = 0) \equiv A_1(0)$, $A_2(z = 0) \equiv A_2(0)$, $A_3(0) = A_3^*(0)$ is

$$A_1(z) = A_1(0)\cosh\frac{g}{2}z - iA_2^*(0)\sinh\frac{g}{2}z$$
$$A_2^*(z) = A_2^*(0)\cosh\frac{g}{2}z + iA_1(0)\sinh\frac{g}{2}z \tag{8.6-22}$$

Equations (8.6-22) describe the growth of the signal and idler waves under phase-matching conditions. In the case of parametric amplification the input will consist of the pump (ω_3) wave and one of the other two fields, say, ω_1. In this case $A_2(0) = 0$, and using the relation $N_i \propto A_iA_i^*$ for the photon flux we obtain from (8.6-22)

$$N_1(z) \propto A_1^*(z)A_1(z) = |A_1(0)|^2\cosh^2\frac{gz}{2} \xrightarrow[gz\gg 1]{} \frac{|A_1(0)|^2}{4}e^{gz}$$
$$N_2(z) \propto A_2^*(z)A_2(z) = |A_1(0)|^2\sinh^2\frac{gz}{2} \xrightarrow[gz\gg 1]{} \frac{|A_1(0)|^2}{4}e^{gz} \tag{8.6-23}$$

Thus, for $gz \gg 1$, the photon fluxes at ω_1 and ω_2 grow exponentially. If we limit our attention to the wave at ω_1, it undergoes an amplification by a factor

$$\frac{A_1^*(z)A_1(z)}{A_1^*(0)A_1(0)} \underset{gz \gg 1}{=} \tfrac{1}{4}e^{gz} \tag{8.6-24}$$

Numerical Example: Parametric Amplification

The magnitude of the gain coefficient g available in a traveling-wave parametric interaction is estimated for the following case involving the use of a $LiNbO_3$ crystal.

$$d_{311} = 5 \times 10^{-23} \text{ MKS} \quad \text{(see Table 8-1)}$$
$$\nu_1 \cong \nu_2 = 3 \times 10^{14} \text{ Hz}$$
$$P_3/\text{Area} = (\text{pump power}) = 5 \times 10^6 \text{ W/cm}^2$$
$$n_1 \simeq n_2 = 2.2$$

Converting P_3 to $|E_3|^2$ with the use of (8.6-16) and then substituting in (8.6-21), yields

$$g = 0.7 \text{ cm}^{-1}$$

This shows that traveling-wave parametric amplification is not expected to lead to large values of gain except for extremely large pump-power densities. The main attraction of the parametric amplification just described is probably in giving rise to parametric oscillation, which will be described in Section 8.8.

8.7 PHASE-MATCHING IN PARAMETRIC AMPLIFICATION

In the preceding section the analysis of parametric amplification assumed that the phase-matching condition

$$k_3 = k_1 + k_2 \tag{8.7-1}$$

is satisfied. It is important to determine the consequences of violating this condition. We start with equations (8.6-18) taking the loss coefficients $\alpha_1 = \alpha_2 = 0$:

$$\frac{dA_1}{dz} = -i\frac{g}{2}A_2^* e^{-i(\Delta k)z}$$
$$\frac{dA_2^*}{dz} = +i\frac{g}{2}A_1 e^{i(\Delta k)z} \tag{8.7-2}$$

The solution of (8.7-2) is facilitated by the substitution

$$A_1(z) = m_1 e^{[s - i(\Delta k/2)]z}$$
$$A_2^*(z) = m_2 e^{[s + i(\Delta k/2)]z} \tag{8.7-3}$$

where m_1 and m_2 are coefficients independent of z. The exponential growth constant s is to be determined. Substitution of (8.7-3) in (8.7-2) leads to

$$\left(s - i\frac{\Delta k}{2}\right) m_1 + i\frac{g}{2} m_2 = 0$$
$$-i\frac{g}{2} m_1 + \left(s + i\frac{\Delta k}{2}\right) m_2 = 0 \tag{8.7-4}$$

By equating the determinant of the coefficients of m_1 and m_2 in (8.7-4) to zero, we obtain the two solutions

$$s_\pm = \pm\tfrac{1}{2}\sqrt{g^2 - (\Delta k)^2} \equiv \pm b \tag{8.7-5}$$

The general solution of (8.7-2) is the sum of the two independent solutions

$$A_1(z) = m_1^+ e^{[s_+ - i(\Delta k/2)]z} + m_1^- e^{[s_- - i(\Delta k/2)]z}$$
$$A_2^*(z) = m_2^+ e^{[s_+ + i(\Delta k/2)]z} + m_2^- e^{[s_- + i(\Delta k/2)]z} \tag{8.7-6}$$

The coefficients m_1^+, m_1^-, m_2^+, m_2^- are next determined by requiring that at $z = 0$ the solution (8.7-6) agree with the input amplitudes $A_1(0)$ and $A_2^*(0)$. This leads straightforwardly to the result

$$A_1(z)e^{i(\Delta k/2)z} = A_1(0)\left[\cosh(bz) + \frac{i(\Delta k)}{2b}\sinh(bz)\right] - i\frac{g}{2b} A_2^*(0)\sinh(bz)$$
$$A_2^*(z)e^{-i(\Delta k/2)z} = A_2^*(0)\left[\cosh(bz) - \frac{i(\Delta k)}{2b}\sinh(bz)\right] + i\frac{g}{2b} A_1(0)\sinh(bz) \tag{8.7-7}$$

The last result reduces, as it should, to (8.6-22) if we put $\Delta k = 0$.

The most noteworthy feature of (8.7-5) and (8.7-7) is that the exponential gain coefficient b is a function of Δk and that unless

$$g \geqq \Delta k \tag{8.7-8}$$

no sustained growth of the signal (A_1) and idler (A_2) waves is possible, since in this case the cosh and sinh functions in (8.7-7) become

$$\sin\{\tfrac{1}{2}[(\Delta k)^2 - g^2]^{1/2}z\}$$
$$\cos\{\tfrac{1}{2}[(\Delta k)^2 - g^2]^{1/2}z\}$$

respectively, and the energies at ω_1 and ω_2 oscillate as a function of the distance z.

The problem of phase-matching in parametric amplification is fundamentally the same as that in second-harmonic generation. Instead of satisfying the condition (8.3-6), $k^{2\omega} = 2k^{\omega}$, we have, according to (8.7-1), to satisfy the condition

$$k_3 = k_1 + k_2$$

This is done, as in second-harmonic generation, by using the dependence of the phase velocity of the extraordinary wave in axial crystals on the direction of propagation. In a negative uniaxial crystal ($n_e < n_0$), we can, as an example, choose the signal and idler waves as ordinary while the pump at ω_3 is applied as an extraordinary wave. Using (8.3-11) and the relation $k^{\omega} = (\omega/c)n^{\omega}$, the phase-matching condition (8.7-1) is satisfied when all three waves propagate at an angle θ_m to the z (optic) axis where

$$n_e^{\omega_3}(\theta_m) = \left[\left(\frac{\cos\theta_m}{n_o^{\omega_3}}\right)^2 + \left(\frac{\sin\theta_m}{n_e^{\omega_3}}\right)^2\right]^{-1/2} = \frac{\omega_1}{\omega_3} n_o^{\omega_1} + \frac{\omega_2}{\omega_3} n_o^{\omega_2} \qquad (8.7\text{-}9)$$

8.8 PARAMETRIC OSCILLATION[11]

In the two preceding sections we have demonstrated that a pump wave at ω_3 can cause a simultaneous amplification in a nonlinear medium of "signal" and "idler" waves at frequencies ω_1 and ω_2, respectively, where $\omega_3 = \omega_1 + \omega_2$. If the nonlinear crystal is placed within an optical resonator (as shown in Figure 8-16) that provides resonances for the signal or idler waves (or both), the parametric gain will, at some threshold pumping intensity, cause a simultaneous oscillation at the signal and idler frequencies. The threshold pumping corresponds to the point at which the parametric gain just balances the losses of the signal and idler waves. This is the physical basis of the optical parametric oscillator. Its practical importance derives from its ability

[11] See References [14–16].

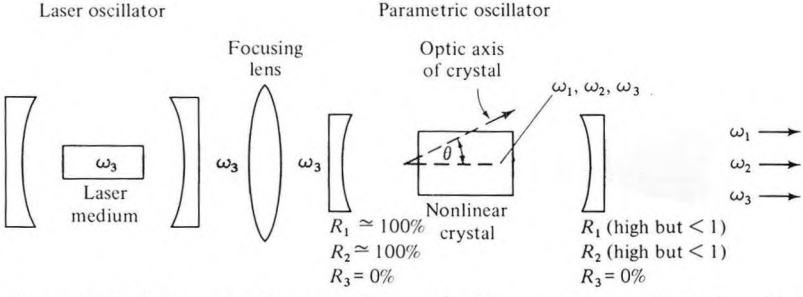

Figure 8-16 Schematic diagram of an optical parametric oscillator in which the laser output at ω_3 is used as the pump, giving rise to oscillations at ω_1 and ω_2 (where $\omega_3 = \omega_1 + \omega_2$) in an optical cavity that contains the nonlinear crystal and resonates at ω_1 and ω_2.

to convert the power output of the pump laser to power at the signal and idler frequencies that, as will be shown below, can be tuned continuously over large ranges.

To analyze this situation we return to (8.6-18). We take $\Delta k = 0$ and neglect the depletion of the pump waves, so $A_3(z) = A_3(0)$. The result is

$$\frac{dA_1}{dz} = -\frac{1}{2}\alpha_1 A_1 - i\frac{g}{2}A_2^*$$
$$\frac{dA_2^*}{dz} = -\frac{1}{2}\alpha_2 A_2^* + i\frac{g}{2}A_1 \qquad (8.8\text{-}1)$$

where, as in (8.6-21),

$$g \equiv \sqrt{\left(\frac{\mu}{\epsilon_0}\right)\frac{\omega_1\omega_2}{n_1 n_2}}\, dE_3(0)$$
$$\alpha_{1,2} \equiv \sigma_{1,2}\sqrt{\frac{\mu}{\epsilon_{1,2}}} \qquad (8.8\text{-}2)$$

Equations (8.8-1) describe traveling-wave parametric interaction. We will use them to describe the interaction inside a resonator such as the one shown in Figure 8-16. This procedure seems plausible if we think of propagation inside an optical resonator as a folded optical path. The magnitude of the spatial distributed loss constants α_1 and α_2 must then be chosen so that they account for the actual losses in the resonator. The latter will include losses caused by the less than perfect reflection at the mirrors, as well as distributed loss in the nonlinear crystal and that due to diffraction.[12]

If the parametric gain is sufficiently high to overcome the losses, steady-state oscillation results. When this is the case,

$$\frac{dA_1}{dz} = \frac{dA_2^*}{dz} = 0 \qquad (8.8\text{-}3)$$

and thus the power gained via the parametric interaction just balances the losses.

Putting $d/dz = 0$ in (8.8-1) gives

$$-\frac{\alpha_1}{2}A_1 - i\frac{g}{2}A_2^* = 0$$
$$i\frac{g}{2}A_1 - \frac{\alpha_2}{2}A_2^* = 0 \qquad (8.8\text{-}4)$$

The condition for nontrivial solutions for A_1 and A_2^* is that the determinant

[12]The effective loss constant α_i is chosen so that $\exp(-\alpha_i l)$ is the total attenuation in intensity per resonator pass at ω_i, where l is the crystal length.

at (8.8-4) vanish; that is,

$$\det \begin{vmatrix} -\frac{\alpha_1}{2} & -i\frac{g}{2} \\ i\frac{g}{2} & -\frac{\alpha_2}{2} \end{vmatrix} = 0$$

and, therefore,

$$g^2 = \alpha_1 \alpha_2 \tag{8.8-5}$$

This is the *threshold condition* for *parametric oscillation.*

If we choose to express the mode losses at ω_1 and ω_2 by the quality factors Q_1 and Q_2, respectively, we have[13]

$$\alpha_i = \frac{\omega_i n_i}{Q_i c} \tag{8.8-6}$$

By the use of (8.8-2), condition (8.8-5) can be written as

$$\frac{d(E_3)_t}{\sqrt{\epsilon_1 \epsilon_2}} = \frac{1}{\sqrt{Q_1 Q_2}} \tag{8.8-7}$$

where $(E_3)_t$ is the value of E_3 at threshold. This relation can be shown to be formally analogous to that obtained in (8.6-10) for the lumped-circuit parametric oscillator. According to (8.6-14), $\Delta C/C_0 = dE_0/\epsilon$; therefore, apart from a factor of two, if we put $Q_1 = Q_2$ and $\epsilon_1 = \epsilon_2$, (8.8-7) is the same as (8.6-10).

Another useful form of the threshold relation results from representing the quality factor Q in terms of the (effective) mirror reflectivities as in (4.7-3) and (4.7-5). If, furthermore, we express E_3 in terms of the power flow per unit area according to (8.6-16)

$$E_3^2 = 2\frac{P_3}{A}\sqrt{\frac{\mu}{\epsilon_0 n_3^2}}$$

we can rewrite (8.8-7) as

$$\left(\frac{P_3}{A}\right)_t = \frac{1}{2}\left(\frac{\epsilon_0}{\mu}\right)^{3/2} \frac{n_1 n_2 n_3 (1 - R_1)(1 - R_2)}{\omega_1 \omega_2 l^2 d^2} \tag{8.8-8}$$

where l is the length of the nonlinear crystal.

---

[13]This relation follows from recognizing that the temporal decay rate $\sigma = \omega/Q$ is related to α by $\sigma = \alpha c/n$.

Numerical Example: Parametric Oscillation Threshold

Let us estimate the threshold pump requirement P_3/A (watts per square centimeter) of a parametric oscillator of the kind shown in Figure 8-16, which utilizes an $LiNbO_3$ crystal. We use the following set of parameters:

$(1 - R_1) = (1 - R_2) = 2 \times 10^{-2}$ (that is, loss per pass at ω_1 and ω_2 = 2 percent)

$(\lambda)_1 = (\lambda)_2 = 1\ \mu m$

$l = 5$ cm (crystal length)

$n_1 = n_2 = n_3 = 1.5$

$d_{311}(LiNbO_3) = 5 \times 10^{-23}$

Substitution in (8.8-8) yields

$$\left(\frac{P_3}{A}\right)_t \cong 50 \text{ watts/cm}^2$$

This is a modest amount of power so that the example helps us appreciate the attractiveness of optical parametric oscillation as a means for generating coherent optical frequency at new optical frequencies.

8.9 FREQUENCY TUNING IN PARAMETRIC OSCILLATION

We have shown above that the pair of signals (ω_1) and idler frequencies that are caused to oscillate by parametric pumping at ω_3 satisfy the condition $k_3 = k_1 + k_2$. Using $k_i = \omega_i n_i/c$ we can write it as

$$\omega_3 n_3 = \omega_1 n_1 + \omega_2 n_2 \qquad (8.9\text{-}1)$$

In a crystal the indices of refraction generally depend, as shown in Section 8.3, on the frequency, crystal orientation (if the wave is extraordinary), electric field (in electrooptic crystals), and on the temperature. If, as an example, we change the crystal orientation in the oscillator shown in Figure 8-16, the oscillation frequencies ω_1 and ω_2 will change so as to compensate for the change in indices, and thus condition (8.9-1) will be satisfied at the new frequencies.

To be specific, we consider the case of a parametric oscillator pumped by an extraordinary beam at a fixed frequency ω_3. The signal (ω_1) and the idler (ω_2) are ordinary waves. At some crystal orientation θ_0 the oscillation takes place at frequencies ω_{10} and ω_{20}. Let the indices of refraction at ω_{10}, ω_{20}, and ω_{30} under those conditions be n_{10}, n_{20}, and n_{30}, respectively. We

want to find the change in ω_1 and ω_2 due to a small change $\Delta\theta$ in the crystal orientation.

From (8.9-1) we have, at $\theta = \theta_0$,

$$\omega_3 n_{30} = \omega_{10} n_{10} + \omega_{20} n_{20} \tag{8.9-2}$$

After the crystal orientation has been changed from θ_0 to $\theta_0 + \Delta\theta$, the following changes occur:

$$\begin{aligned} n_{30} &\to n_{30} + \Delta n_3 \\ n_{10} &\to n_{10} + \Delta n_1 \\ n_{20} &\to n_{20} + \Delta n_2 \\ \omega_{10} &\to \omega_{10} + \Delta\omega_1 \end{aligned}$$

Since $\omega_1 + \omega_2 = \omega_3 = \text{constant}$,

$$\omega_{20} \to \omega_{20} + \Delta\omega_2 = \omega_{20} - \Delta\omega_1$$

that is, $\Delta\omega_2 = -\Delta\omega_1$. Since (8.9-1) must be satisfied at $\theta = \theta_0 + \Delta\theta$, we have

$$\omega_3(n_{30} + \Delta n_3) = (\omega_{10} + \Delta\omega_1)(n_{10} + \Delta n_1) + (\omega_{20} - \Delta\omega_1)(n_{20} + \Delta n_2)$$

Neglecting the second-order terms $\Delta n_1 \Delta\omega_1$ and $\Delta n_2 \Delta\omega_1$ and using (8.9-2), we obtain

$$\Delta\omega_1 \bigg|_{\substack{\omega_1 \simeq \omega_{10} \\ \omega_2 \simeq \omega_{20}}} = \frac{\omega_3 \Delta n_3 - \omega_{10} \Delta n_1 - \omega_{20} \Delta n_2}{n_{10} - n_{20}} \tag{8.9-3}$$

According to our starting hypotheses the pump is an extraordinary ray; therefore, according to (1.4-12), its index depends on the orientation θ, giving

$$\Delta n_3 = \frac{\partial n_3}{\partial \theta}\bigg|_{\theta_0} \Delta\theta \tag{8.9-4}$$

The signal and idler are ordinary rays, so their indices depend on the frequencies but not on the direction. It follows that

$$\begin{aligned} \Delta n_1 &= \frac{\partial n_1}{\partial \omega_1}\bigg|_{\omega_{10}} \Delta\omega_1 \\ \Delta n_2 &= \frac{\partial n_2}{\partial \omega_2}\bigg|_{\omega_{20}} \Delta\omega_2 \end{aligned} \tag{8.9-5}$$

Using the last two equations in (8.9-3) results in

$$\frac{\partial \omega_1}{\partial \theta} = \frac{\omega_3(\partial n_3/\partial\theta)}{(n_{10} - n_{20}) + [\omega_{10}(\partial n_1/\partial\omega_1) - \omega_{20}(\partial n_2/\partial\omega_2)]} \tag{8.9-6}$$

for the rate of change of the oscillation frequency with respect to the crystal

orientation. Using (1.4-12) and the relation $d(1/x^2) = -(2/x^3)\,dx$, we obtain

$$\frac{\partial n_3}{\partial \theta} = -\frac{n_3^3}{2}\sin(2\theta)\left[\left(\frac{1}{n_e^{\omega_3}}\right)^2 - \left(\frac{1}{n_o^{\omega_3}}\right)^2\right]$$

which, when substituted in (8.9-6), gives

$$\frac{\partial \omega_1}{\partial \theta} = \frac{-\frac{1}{2}\,\omega_3 n_{30}^3\left[\left(\frac{1}{n_e^{\omega_3}}\right)^2 - \left(\frac{1}{n_o^{\omega_3}}\right)^2\right]\sin(2\theta)}{(n_{10} - n_{20}) + \left(\omega_{10}\frac{\partial n_1}{\partial \omega_1} - \omega_{20}\frac{\partial n_2}{\partial \omega_2}\right)} \tag{8.9-7}$$

An experimental curve showing the dependence of the signal and idler frequencies on θ in $NH_4H_2PO_4$ (ADP) is shown in Figure 8-17. Also shown is a theoretical curve based on a quadratic approximation of (8.9-7), which was plotted using the dispersion (that is, n versus ω) data of ADP; see Reference [17].

Reasoning similar to that used to derive the angle-tuning expression (8.9-7) can be applied to determine the dependence of the oscillation frequency on temperature. Here we need to know the dependence of the various indices on temperature. This is discussed further in Problem 8-6. An experimental temperature-tuning curve is shown in Figure 8-18.

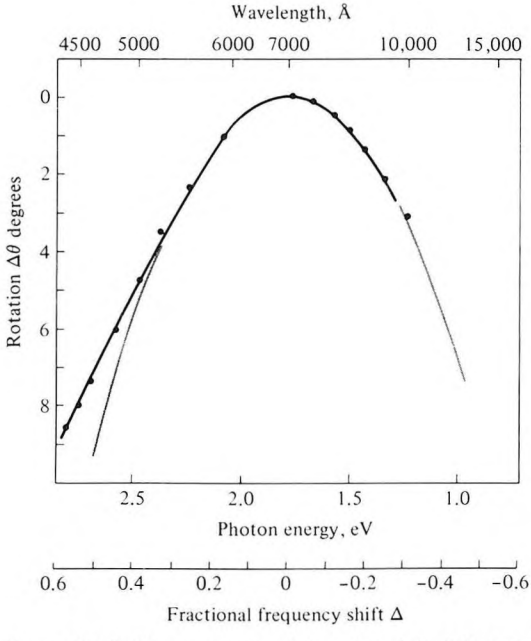

Figure 8-17 Dependence of the signal (ω_1) frequency on the angle between the pump propagation direction and the optic axis of the ADP crystal. The angle θ is measured with respect to the angle for which $\omega_1 = \omega_3/2$. $\Delta \equiv (\omega_1 - \omega_3/2)/(\omega_3/2)$. (After Reference [17].)

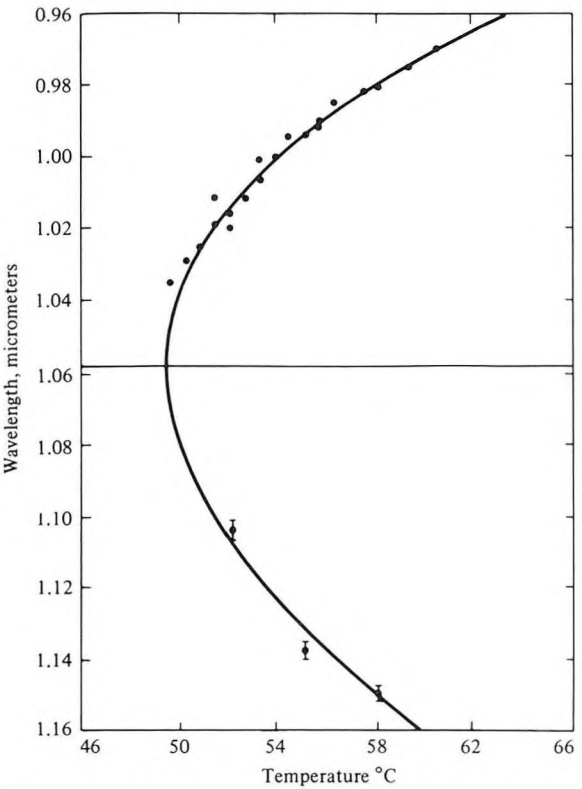

Figure 8-18 Signal and idler wavelength as a function of the temperature of the oscillator crystal. (After Reference [15].)

8.10 POWER OUTPUT AND PUMP SATURATION IN OPTICAL PARAMETRIC OSCILLATORS

In the treatment of the laser oscillator in Section 6.5 we showed that in the steady state the gain could not exceed the threshold value regardless of the intensity of the pump. A closely related phenomenon exists in the case of parametric oscillation. The pump field E_3 gives rise to amplification of the signal and idler waves. When E_3 reaches its critical (threshold) value given by (8.8-7), the gain just equals the losses and the device is on the threshold of oscillation. If the pump field E_3 is increased beyond its threshold value, the gain can no longer follow it and must be "clamped" at its threshold value. This follows from the fact that if the gain constant g exceeds its threshold value (8.8-5), a steady state is no longer possible and the signal and idler intensities will increase with time. Since the gain g is proportional to the pump field E_3, it follows that above threshold the *pump field inside* the optical resonator must saturate at its level just prior to oscillation. As power is conserved it follows that any additional pump power input must

be diverted into power at the signal and idler fields. Since $\omega_3 = \omega_1 + \omega_2$, it follows that for each input pump photon above threshold we generate one photon at the signal (ω_1) and one at the idler (ω_2) frequencies, so [18]

$$\frac{P_1}{\omega_1} = \frac{P_2}{\omega_2} = \frac{(P_3)_t}{\omega_3}\left(\frac{P_3}{(P_3)_t} - 1\right) \tag{8.10-1}$$

The last argument shows that in principle the parametric oscillator can attain high efficiencies. This requires operation well above threshold, and thus $P_3/(P_3)_t \gg 1$. These considerations are borne out by actual experiments [19].

Figure 8-19 shows experimental confirmation of the phenomenon of pump saturation; see References [18, 21]. After a transient buildup the pump intensity inside the resonator settles down to its threshold value.

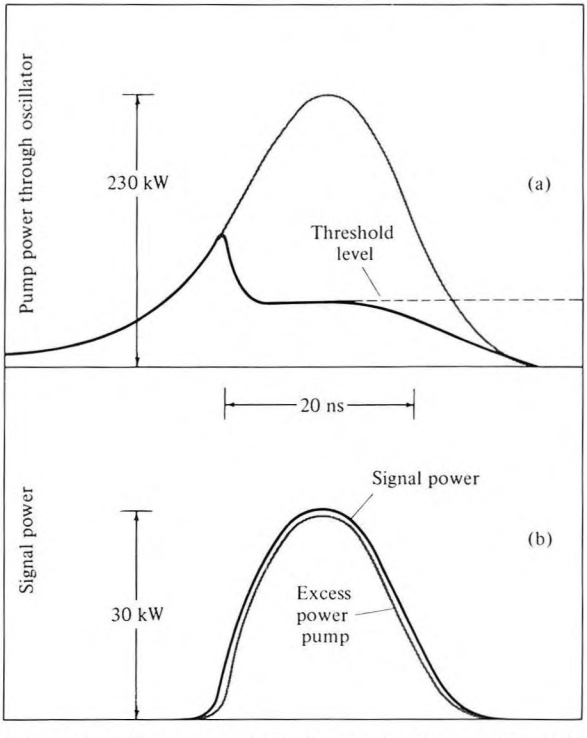

Figure 8-19 Power levels and pumping in a parametric oscillator. (a) Waveforms of P_3, the pump power passing through the oscillator. The gray waveform was obtained when the crystal was rotated so that oscillation did not occur; the solid waveform was obtained when oscillation took place. (b) Signal power and excess pump power. The gray waveform is the normalized difference between the waveforms in (a). (After Reference [19].)

Figure 8-19(b) shows that the signal power is proportional to the excess (above threshold) pump input power. This is in agreement with Equation (8.10-1).

8.11 FREQUENCY UP-CONVERSION

Parametric interactions in a crystal can be used to convert a signal from a "low" frequency ω_1 to a "high" frequency ω_3 by mixing it with a strong laser beam at ω_2, where

$$\omega_1 + \omega_2 = \omega_3 \tag{8.11-1}$$

Using the quantum mechanical photon picture described in Section 8.5, we can consider the basic process taking place in frequency up-conversion as one in which a signal (ω_1) photon and a pump (ω_2) photon are annihilated while, simultaneously, one photon at ω_3 is generated; see References [12, 22–25]. Since a photon energy is $h\omega$, conservation of energy dictates that $\omega_3 = \omega_1 + \omega_2$ and, in a manner similar to (8.5-1), the conservation of momentum leads to the relationship

$$\mathbf{k}_3 = \mathbf{k}_1 + \mathbf{k}_2 \tag{8.11-2}$$

between the wave vectors at the three frequencies. This point of view also suggests that the number of output photons at ω_3 cannot exceed the input number of photons at ω_1.

The experimental situation is demonstrated by Figure 8-20. The ω_1 and ω_2 beams are combined in a partially transmissive mirror (or prism), so they traverse together (in near parallelism) the length l of a crystal possessing nonlinear optical characteristics.

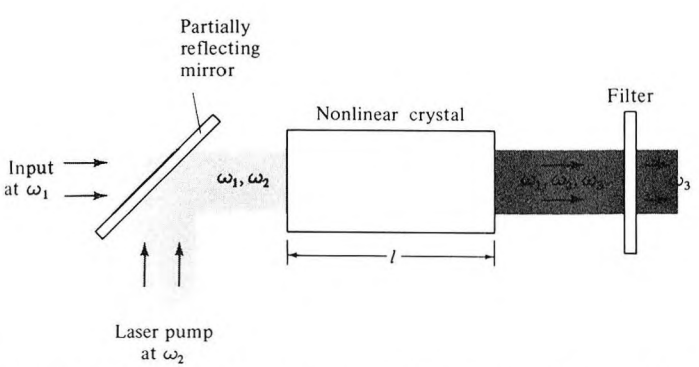

Figure 8-20 Parametric up-conversion in which a signal at ω_1 and a strong laser beam at ω_2 combine in a nonlinear crystal to generate a beam at the sum frequency $\omega_3 = \omega_1 + \omega_2$.

The analysis of frequency up-conversion starts with Equation (8.6-18). Assuming negligible depletion of the pump wave A_2, no losses ($\alpha = 0$) at ω_1 and ω_3, and taking $\Delta k = 0$, we can write the first and third of these equations as

$$\frac{dA_1}{dz} = -i\frac{g}{2}A_3$$
$$\frac{dA_3}{dz} = -i\frac{g}{2}A_1 \qquad (8.11\text{-}3)$$

where, using (8.6-15) and (8.6-19) and choosing without loss of generality the pump phase as zero so that $A_2(0) = A_2^*(0)$,

$$g \equiv \sqrt{\frac{\omega_1\omega_3}{n_1 n_3}\left(\frac{\mu}{\epsilon_0}\right)}\, dE_2 \qquad (8.11\text{-}4)$$

where E_2 is the amplitude of the electric field of the pump laser. Taking the input waves with (complex) amplitudes $A_1(0)$ and $A_3(0)$, the general solution of (8.11-3) is

$$A_1(z) = A_1(0)\cos\left(\frac{g}{2}z\right) - iA_3(0)\sin\left(\frac{g}{2}z\right)$$
$$A_3(z) = A_3(0)\cos\left(\frac{g}{2}z\right) - iA_1(0)\sin\left(\frac{g}{2}z\right) \qquad (8.11\text{-}5)$$

In the case of a single (low) frequency input at ω_1, we have $A_3(0) = 0$. In this case,

$$|A_1(z)|^2 = |A_1(0)|^2\cos^2\left(\frac{g}{2}z\right)$$
$$|A_3(z)|^2 = |A_1(0)|^2\sin^2\left(\frac{g}{2}z\right) \qquad (8.11\text{-}6)$$

therefore,

$$|A_1(z)|^2 + |A_3(z)|^2 = |A_1(0)|^2$$

In the discussion following (8.6-17) we pointed out that $|A_l(z)|^2$ is proportional to the photon flux (photons per square meter per second) at ω_l. Using this fact we may interpret (8.11-6) as stating that the photon flux at ω_1 plus that at ω_3 at any plane z is a constant equal to the input ($z = 0$) flux at ω_1. If we rewrite (8.11-6) in terms of powers, we obtain

$$P_1(z) = P_1(0)\cos^2\left(\frac{g}{2}z\right)$$
$$P_3(z) = \frac{\omega_3}{\omega_1}P_1(0)\sin^2\left(\frac{g}{2}z\right) \qquad (8.11\text{-}7)$$

In a crystal of length l, the conversion efficiency is thus

$$\frac{P_3(l)}{P_1(0)} = \frac{\omega_3}{\omega_1} \sin^2\left(\frac{g}{2} l\right) \tag{8.11-8}$$

and can have a maximum value of ω_3/ω_1, corresponding to the case in which all the input (ω_1) photons are converted to ω_3 photons.

In most practical situations the conversion efficiency is small (see the following numerical example) so using $\sin x \simeq x$ for $x \ll 1$, we get

$$\frac{P_3(l)}{P_1(0)} \simeq \frac{\omega_3}{\omega_1}\left(\frac{g^2 l^2}{4}\right)$$

which, by the use of (8.11-4) and (8.6-16), can be written as

$$\frac{P_3(l)}{P_1(0)} \simeq \frac{\omega_3^2 l^2 d^2}{2n_1 n_2 n_3}\left(\frac{\mu}{\epsilon_0}\right)^{3/2}\left(\frac{P_2}{A}\right) \tag{8.11-9}$$

where A is the cross-sectional area of the interaction region.

Numerical Example: Frequency Up-Conversion

The main practical interest in parametric frequency up-conversion stems from the fact that it offers a means of detecting infrared radiation (a region where detectors are either inefficient, very slow, or require cooling to cryogenic temperatures) by converting the frequency into the visible or near-visible part of the spectrum. The radiation can then be detected by means of efficient and fast detectors such as photomultipliers or photodiodes; see References [23–26].

As an example of this application, consider the problem of up-converting a 10.6-μm signal, originating in a CO_2 laser to 0.96 μm by mixing it with the 1.06-μm output of an Nd^{3+}:YAG laser. The nonlinear crystal chosen for this application has to have low losses at 1.06 μm and 10.6 μm, as well as at 0.96 μm. In addition, its birefringence has to be such as to make phase matching possible. The crystal proustite (Ag_3AsS_3) listed in Table 8-1 meets these requirements [26].

Using the data

$$\frac{P_{1.06\mu m}}{A} = 10^4 \text{ W/cm}^2 = 10^8 \text{ W/m}^2$$

$$l = 10^{-2} \text{ meter}$$

$$n_1 \simeq n_2 \simeq n_3 = 2.6 \quad \text{(an average number based on the data of Reference [26])}$$

$$d_{\text{eff}} = 1.1 \times 10^{-22} \quad \text{(taken conservatively as a little less than half the value given in Table 8.1 for } d_{22})$$

we obtain, from (8.11-9),

$$\frac{P_{\lambda=0.96\mu m}(l = 1 \text{ cm})}{P_{\lambda=10.6\mu m}(l = 0)} = 7.1 \times 10^{-4}$$

indicating a useful amount of conversion efficiency.

Problems

8.1 Show that if θ_m is the phase-matching angle for an ordinary wave at ω and an extraordinary wave at 2ω, then

$$\Delta k(\theta)l|_{\theta=\theta_m} = -\frac{2\omega l}{c_0} \sin(2\theta_m) \frac{(n_e^{2\omega})^{-2} - (n_o^{2\omega})^{-2}}{2(n_o^{\omega})^{-3}} (\theta - \theta_m)$$

8.2 Derive the expression for the phase-matching angle of a parametric amplifier using KDP in which two of the waves are extraordinary while the third is ordinary. Which of the three waves (that is, signal, idler, or pump) would you choose as ordinary? Can this type of phase-matching be accomplished with $\omega_3 = 10{,}000 \text{ cm}^{-1}$, $\omega_1 = \omega_2 = 5000 \text{ cm}^{-1}$? If so, what is θ_m?

8.3 Show that Equations (8.6-22) are consistent with the fact that the increases in the photon flux at ω_1 and ω_2 are identical—that is, that $A_1^*(z)A_1(z) - A_1^*(0)A_1(0) = A_2^*(z)A_2(z) - A_2^*(0)A_2(0)$.

8.4 Complete the missing steps in the derivation of Equation (8.7-7).

8.5 Show that the voltage $v(t)$ across an open-circuited parallel RLC circuit obeys

$$\frac{d^2v}{dt^2} + \frac{1}{RC}\frac{dv}{dt} + \frac{1}{LC}v = 0$$

and is thus of the form of Equation (8.6-1).

8.6 Consider a parametric oscillator setup such as that shown in Figure 8-15. The crystal orientation angle is θ, its temperature is T, and the signal and idler frequencies are ω_{10} and ω_{20}, respectively, with $\omega_{10} + \omega_{20} = \omega_3$. Show that a small temperature change ΔT causes the signal frequency to change by

$$\Delta\omega_1 = \Delta T \times \left\{ \omega_3 \left[\cos^2\theta \left(\frac{n_e^{\omega_3}(\theta)}{n_0^{\omega_3}} \right)^3 \frac{\partial n_0^{\omega_3}}{\partial T} + \sin^2\theta \left(\frac{n_e^{\omega_3}(\theta)}{n_e^{\omega_3}} \right)^3 \frac{\partial n_e^{\omega_3}}{\partial T} \right] - \omega_{10} \frac{\partial n_o^{\omega_1}}{\partial T} - \omega_{20} \frac{\partial n_o^{\omega_2}}{\partial T} \right\} \times \frac{1}{n_{10} - n_{20}}$$

The pump is taken as an extraordinary ray, whereas the signal and idler are ordinary. [*Hint:* The starting point is Equation (8.9-3), which is valid regardless of the nature of the perturbation.]

8.7 Using the published dispersion data of proustite (Reference [26]), calculate the maximum angular deviation of the input beam at ν_1 (from parallelism with the pump beam at ν_2) that results in a reduction by a factor of 2 in the conversion efficiency. Take $\lambda_1 = 10.6\ \mu$m, $\lambda_2 = 1.06\ \mu$m, $\lambda_3 = 0.964\ \mu$m. [*Hint:* A proper choice must be made for the polarizations at ω_1, ω_2, and ω_3 so that phase-matching can be achieved along some angle.] The maximum angular deviation is that for which

$$\frac{\sin^2[\Delta k(\theta)l/2]}{[\Delta k(\theta)l/2]^2} = \frac{1}{2}$$

where, at the phase-matching angle θ_m, $\Delta k(\theta_m) = 0$. Approximate the dispersion data by a Taylor-series expansion about the nominal ($\Delta k = 0$) frequencies.

8.8 Using the dispersion data of Reference [26], discuss what happens to phase-matching in an up-conversion experiment due to a deviation of the input frequency from the nominal ($\Delta k = 0$)ν_{10} value. Derive an expression for the spectral width of the output in the case where the input spectral density (power per unit frequency) in the vicinity of ν_{10} is uniform. [*Hint:* Use a Taylor-series expansion of the dispersion data about the phase-matching ($\Delta k = 0$) frequencies to obtain an expression for $\Delta k(\nu_3)$.] Define the output spectral width as twice the frequency deviation at which the output is half its maximum ($\Delta k = 0$) value.

8.9 Explain using qualitative reasoning why (8.6-5) admits $\phi = 0$ and $\phi = \pi$ solutions.

8.10 Show that if the nonlinear optical constant is spatially periodic, i.e.,

$$d = \frac{d_0}{2}(e^{ikz} + e^{-ikz})$$

then a proper choice of the period $2\pi/k$ can lead to phase-matched operation. [*Hint:* Try Equation (8.2-13) and justify the neglect of terms with nonzero exponents compared with phase-matched terms (where the exponent is zero).] This method of phase-matching is referred to as quasi phase-matching [27–29].

8.11 Applying the transformation rule $d_{ij} \leftrightarrow r_{ji}$ from Section 8.1, generate the symmetry table d_{ij} of KH_2PO_4. Compare the result to that of Equation (8.1-19a).

References

1. Miller, R. C., "Optical second harmonic generation in piezoelectric crystals," *Appl. Phys. Lett.* 5:17, 1964.
2. Garret, C. G. B., and F. N. H. Robinson, "Miller's phenomenological

rule for computing nonlinear susceptibilities," *IEEE J. Quant. Elec.* QE-2:328, 1966.

3. See, for example, J. F. Nye, *Physical Properties of Crystals*. New York: Oxford, 1957.
4. Armstrong, J. A., N. Bloembergen, J. Ducuing, and P. S. Pershan, "Interactions between light waves in a nonlinear dielectric," *Phys. Rev.* 127:1918, 1962.
5. Franken, P. A., A. E. Hill, C. W. Peters, and G. Weinreich, "Generation of optical harmonics," *Phys. Rev. Lett.* 7:118, 1961.
6. Maker, P. D., R. W. Terhune, M. Nisenoff, and C. M. Savage, "Effects of dispersion and focusing on the production of optical harmonics," *Phys. Rev. Lett.* 8:21, 1962.
7. Giordmaine, J. A., "Mixing of light beams in crystals," *Phys. Rev. Lett.* 8:19, 1962.
8. Zernike, F., Jr., "Refractive indices of ammonium dihydrogen phosphate and potassium dihydrogen phosphate between 2000 Å and 1.5 μ," *J. Opt. Soc. Am.* 54:1215, 1964.
9. Thorsos, E. I., ed. *Laboratory for Laser Analytics Review*, vol. II, p. 7, 1979–1980.
10. Geusic, J. E., H. J. Levinstein, S. Singh, R. G. Smith, and L. G. Van Uitert, "Continuous 0.53-μm solid-state source using $Ba_2NaNb_5O_{15}$," *IEEE J. Quant. Elec.* QE-4:352, 1968.
11. Ashkin, A., G. D. Boyd, and J. M. Dziedzic, "Observation of continuous second harmonic generation with gas lasers," *Phys. Rev. Lett.* 11:14, 1963.
12. Yariv, A., *Quant. Elec.* 3rd ed. New York: Wiley, 1989.
13. Lord Rayleigh, "On maintained vibrations," *Phil. Mag.*, vol. 15, ser. 5, pt. I, p. 229, 1883.
14. Parametric amplification was first demonstrated by C. C. Wang and G. W. Racette, "Measurement of parametric gain accompanying optical difference frequency generation," *Appl. Phys. Lett.* 6:169, 1965.
15. The first demonstration of optical parametric oscillation is that of J. A. Giordmaine and R. C. Miller, "Tunable optical parametric oscillation in $LiNbO_3$ at optical frequencies," *Phys. Rev. Lett.* 14:973, 1965.
16. Some of the early theoretical analyses of optical parametric oscillation are attributable to R. H. Kingston, "Parametric amplification and oscillation at optical frequencies," *Proc. IRE* 50:472, 1962, and N. M. Kroll, "Parametric amplification in spatially extended media and applications to the design of tunable oscillators at optical frequencies," *Phys. Rev.* 127:1207, 1962.
17. Magde, D., and H. Mahr, "Study in ammonium dihydrogen phosphate of spontaneous parametric interaction tunable from 4400 to 16000 Å," *Phys. Rev. Lett.* 18:905, 1967.
18. Yariv, A., and W. H. Louisell, "Theory of the optical parametric oscillator," *IEEE J. Quant. Elec.* QE-2:418, 1966.

19. Bjorkholm, J. E., "Efficient optical parametric oscillation using doubly and singly resonant cavities," *Appl. Phys. Lett.* 13:53, 1968.
20. Kreuzer, L. B., "High-efficiency optical parametric oscillation and power limiting in $LiNbO_3$," *Appl. Phys. Lett.* 13:57, 1968.
21. Siegman, A. E., "Nonlinear optical effects: An optical power limiter," *Appl. Opt.* 1:739, 1962.
22. Louisell, W. H., A. Yariv, and A. E. Siegman, "Quantum fluctuations and noise in parametric processes," *Phys. Rev.* 124:1646, 1961.
23. Johnson, F. M., and J. A. Durado, "Frequency up-conversion," *Laser Focus* 3:31, 1967.
24. Midwinter, J. E., and J. Warner, "Up-conversion of near infrared to visible radiation in lithium-meta-niobate," *J. Appl. Phys.* 38:519, 1967.
25. Warner, J., "Photomultiplier detection of 10.6 μ radiation using optical up-conversion in proustite," *Appl. Phys. Lett.* 12:222, 1968.
26. Hulme, K. F., O. Jones, P. H. Davies, and M. V. Hobden, "Synthetic proustite (Ag_3AsS_3): A new material for optical mixing," *Appl. Phys. Lett.* 10:133, 1967.
27. Somekh, S., and A. Yariv, "Phase matching by periodic modulation of the nonlinear optical properties," *Opt. Commun.* 6(3):301, 1972.
28. Somekh, S., and A. Yariv, "Phase matchable nonlinear optical interactions in periodic thin films," *Appl. Phys. Lett.* 21:140, 1972.
29. Bierlein, J. D., D. B. Laubacher, J. B. Brown, and C. J. van der Poel, "Balanced phase matching in segmented KT_iOPO_4 waveguides," *Appl. Phys. Lett.* 56:1725, 1990.

Supplementary References

30. Seka, W., S. D. Jacobs, J. E. Rizzo, R. Boni, and R. S. Craxton, "Demonstration of high efficiency third harmonic conversion of high power Nd-glass laser radiation," *Optics Commun.* 34:469, 1980. Also Craxton, R. S., "High efficiency frequency tripling schemes for high power Nd: glass lasers," *IEEE J. Quant. Elec.* QE-17:177, 1981. (Additional articles on doubling and frequency conversion are to be found in the same issue.)
31. Holzrichter, J. F., D. Eimerl, E. V. George, J. B. Trenholme, W. W. Simmons, and J. T. Hunt, *Physics of Laser Fusion*, vol. III. Lawrence Livermore National Laboratory, September 1982. For availability, see Supplementary Reference [32].
32. George, E. V., ed., *1981 Laser Program Annual Report—Lawrence Livermore Laboratory*, Chapter 7. (Available from the National Technical Information Service, U.S. Department of Commerce, Springfield, VA 22161.)